



LUND UNIVERSITY

Alpha-synuclein: pathology, peripheral expression, and environmental interactions

Haikal, Caroline

2022

Document Version:

Publisher's PDF, also known as Version of record

[Link to publication](#)

Citation for published version (APA):

Haikal, C. (2022). *Alpha-synuclein: pathology, peripheral expression, and environmental interactions*. [Doctoral Thesis (compilation), Department of Experimental Medical Science]. Lund University, Faculty of Medicine.

Total number of authors:

1

General rights

Unless other specific re-use rights are stated the following general rights apply:

Copyright and moral rights for the publications made accessible in the public portal are retained by the authors and/or other copyright owners and it is a condition of accessing publications that users recognise and abide by the legal requirements associated with these rights.

- Users may download and print one copy of any publication from the public portal for the purpose of private study or research.
- You may not further distribute the material or use it for any profit-making activity or commercial gain
- You may freely distribute the URL identifying the publication in the public portal

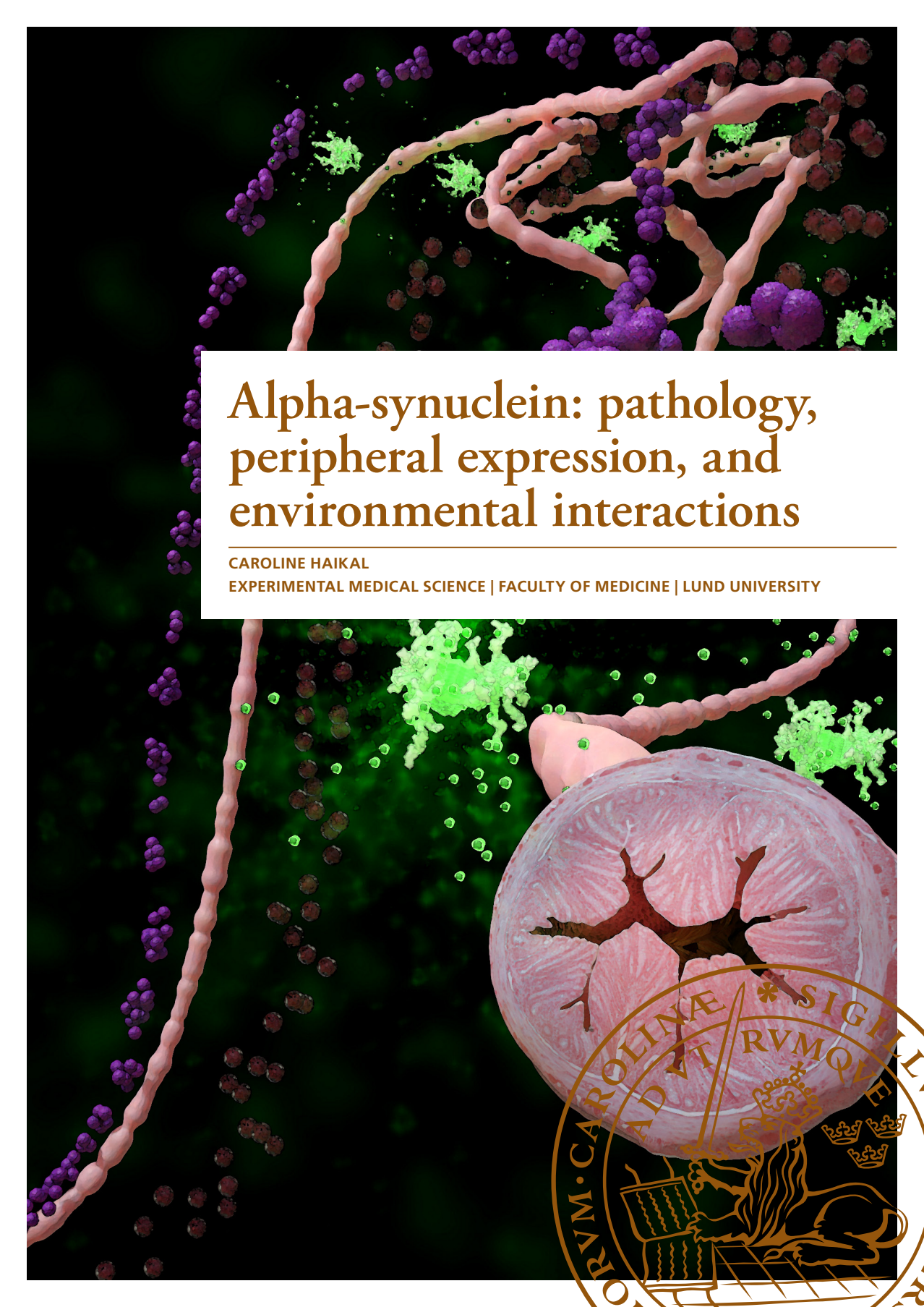
Read more about Creative commons licenses: <https://creativecommons.org/licenses/>

Take down policy

If you believe that this document breaches copyright please contact us providing details, and we will remove access to the work immediately and investigate your claim.

LUND UNIVERSITY

PO Box 117
221 00 Lund
+46 46-222 00 00

A 3D visualization of alpha-synuclein pathology. The background is dark green. There are several long, pink, wavy, rope-like structures representing fibrils. Interspersed among these are numerous small, purple, spherical clusters and some larger, bright green, irregular clusters. In the lower right, there is a large, pink, spherical structure with a brown, branching, tree-like pattern inside it. In the bottom right corner, there is a circular gold seal with Latin text and a central figure.

Alpha-synuclein: pathology, peripheral expression, and environmental interactions

CAROLINE HAIKAL

EXPERIMENTAL MEDICAL SCIENCE | FACULTY OF MEDICINE | LUND UNIVERSITY

Alpha-synuclein: pathology, peripheral expression, and environmental interactions

Caroline Haikal



LUND
UNIVERSITY

DOCTORAL DISSERTATION

by due permission of the Faculty of Medicine, Lund University, Sweden.
To be defended in Segerfalksalen, BMC A10, on March 11th, 2022 at 13:00.

Faculty opponent

Professor Michael Schlossmacher

University of Ottawa, Brain and Mind Research Institute, Canada

Organization LUND UNIVERSITY Faculty of Medicine Dept of Experimental Medical Science Neural Plasticity and Repair Unit		Document name Doctoral thesis	
		Date of issue 11/03/2022	
Author: Caroline Haikal		Sponsoring organization	
Title and subtitle Alpha-synuclein: pathology, peripheral expression, and environmental interactions			
Abstract <p>Synucleinopathies are common neurodegenerative disorders, examples of which are Parkinson's disease, dementia with Lewy bodies, and multiple system atrophy. Common for the diseases is a pathological accumulation and aggregation of the protein alpha-synuclein. Alpha-synuclein can be post-translationally modified and increasing evidence suggests C-terminal truncation plays a role in disease. In our first study we have compared alpha-synuclein in different brain regions from patients with different synucleinopathies. We report that alpha-synuclein is C-terminally truncated to a greater extent in PD than in MSA. We also see differences in alpha-synuclein in different brain regions within the same patient, indicating alpha-synuclein is not homogeneously processed. This could have implications for the design of immunotherapies targeting alpha-synuclein.</p> <p>Additionally, synucleinopathy patients often report gastrointestinal disturbances many years prior to diagnosis. As such, we investigated enteric alpha-synuclein expression in a transgenic mouse model of synucleinopathy. Importantly, this mouse overexpresses human alpha-synuclein under the mouse's endogenous SNCA promotor, meaning the transgene is expressed where endogenous alpha-synuclein is. We found a temporal accumulation of alpha-synuclein in the colon of this mouse: in the submucosa, the mucosa and the myenteric regions. This alpha-synuclein was also increasingly phosphorylated with age. Since the publication of this study, several articles have demonstrated alpha-synuclein in the intestines of patients with synucleinopathy.</p> <p>As these synucleinopathies are often idiopathic in nature, environmental causes have been suspected to underly their initiation. Synucleinopathy patients consistently show altered microbiomes compared to healthy controls. As such, we were interested in studying the effects of bacterial peptides on alpha-synuclein aggregation. We first performed a pilot screen of different bacterial peptides and found that phenol soluble modulins accelerated alpha-synuclein aggregation <i>in vitro</i>. We then further studied the effect of these peptides on alpha-synuclein aggregation and found that these peptides indeed cause the fibrillation of alpha-synuclein as demonstrated by electron microscopy. When alpha-synuclein aggregated in the presence of these peptides was added onto cells, it seeded alpha-synuclein in them. These phenol soluble modulins are expressed by the common bacterium <i>Staphylococcus aureus</i>. We then found that alpha-synuclein accumulated at the site of the lesion in mice infected with <i>S. aureus</i>. Our peptides were dissolved in DMSO. DMSO is a commonly used solvent and is frequently used in aggregation experiments and also as a cryoprotectant for cells. When we studied its effect on alpha-synuclein aggregation we could see that in the presence of other nucleating factors, DMSO accelerated alpha-synuclein aggregation. In cells, even at concentrations as low as 0.25%, compared to 10% usually used for cryoprotection, DMSO induced seeding of alpha-synuclein. When animals were tube-fed with DMSO we did not observe an increase in alpha-synuclein accumulation in the intestines or brain.</p> <p>Elucidating the role and mechanism of α-syn aggregation and the development of better models of synucleinopathies could thus redirect therapeutic and preventative strategies for the different synucleinopathies.</p>			
Key words Alpha-synuclein, neurodegeneration, Parkinson's disease, dementia with Lewy bodies, multiple system atrophy, peripheral expression, bacterial amyloid peptides			
Classification system and/or index terms (if any)			
Supplementary bibliographical information		Language English	
ISSN 1652-8220		ISBN 978-91-8021-201-4	
Recipient's notes		Number of pages 75	
		Price	
		Security classification	

I, the undersigned, being the copyright owner of the abstract of the above-mentioned dissertation, hereby grant to all reference sources permission to publish and disseminate the abstract of the above-mentioned dissertation.

Signature 

Date 2022-02-02

Alpha-synuclein: pathology, peripheral expression, and environmental interactions

Caroline Haikal



LUND
UNIVERSITY

Coverphoto by Andreas Enström

The cover photo is a 3D rendering of an intestine which ends in a cross-section, clusters of *S. aureus* as would be visualized by a gram stain, Lewy bodies as detected by IHC, and green fluorescent alpha-synuclein fibrils

Copyright pp 1-70 (Caroline Haikal)

Paper 1 © by the Authors (Manuscript unpublished)

Paper 2 © by the Authors and Springer Nature

Paper 3 © by the Authors and MDPI

Paper 4 © by the Authors (Manuscript unpublished)

Faculty of Medicine

Department of Experimental Medical Science

ISBN 978-91-8021-201-4

ISSN 1652-8220

Printed in Sweden by Media-Tryck, Lund University
Lund 2022



Media-Tryck is a Nordic Swan Ecolabel
certified provider of printed material.
Read more about our environmental
work at www.mediatryck.lu.se

MADE IN SWEDEN 

To my family,
(and anyone who reads more of this than just the acknowledgements)

Table of Contents

Original articles and manuscripts included in this thesis	8
Published articles not included in this thesis.....	9
Popular science summary	11
Populärvetenskaplig sammanfattning	12
Abbreviations.....	13
Introduction	15
Alpha-synuclein	16
Discovery of alpha-synuclein	16
The synucleins	17
Alpha-synuclein's physiological role	17
Pathology.....	19
Amyloidosis.....	19
A prion-like hypothesis of alpha-synuclein pathology	20
Environmental triggers of alpha-synuclein pathology.....	21
Microbes, the immune system, and neurodegeneration.....	22
Neuroinflammation.....	24
Outlook.....	24
Aims	27
Summary of key results.....	29
Paper I	29
Paper II	34
Paper III.....	38
Paper IV	46
Discussion and Future Perspectives	51

Materials and Methods	55
Human tissues and animal experiments	55
Human post-mortem brain tissue.....	55
Animals	55
Intestinal transit time	55
DMSO administration	56
Tissue sectioning	57
Immunohistochemistry	57
Immunofluorescence	57
Image acquisition.....	59
Biochemical and molecular methods	59
Alpha-synuclein production and purification	59
PSM α peptide production	59
Kinetics experiments	59
Analysis of Kinetics Data	60
Electrophoresis and Mass Spectrometry.....	60
Peptide arrays	60
Transmission Electron Microscopy	61
Dynamic Light Scattering.....	61
Proteinase K digestion and Western Blotting.....	61
Cell Culture	62
SH-SY5Y cells	62
DMSO treatment of SH-SY5Y cells	62
HEK 293T Culture	62
Alpha-synuclein and PSM α treatment of HEK 293T cells	62
References	65
Acknowledgements	75

Original articles and manuscripts included in this thesis

- I. **Haikal, C.**, Liu, D., Brandi, E., Melek Altay, F., Li, W., Englund, E., Lashuel, H.A. & Li, J. Y. Epitope-specific alpha-synuclein pathology in different synucleinopathies (Manuscript)
- II. Chen, Q. Q., **Haikal, C.**, Li W.; Li, M. T., Wang, Z. Y. & Li, J. Y. Age-dependent alpha-synuclein accumulation and aggregation in the colon of a transgenic mouse model of Parkinson's disease. *Translational Neurodegeneration*. 7, 1, 13. (2018). 10.1186/s40035-018-0118-8
- III. **Haikal, C.**, Ortigosa-Pascual, L., Najarzadeh, Z., Bernfur, K., Svanbergsson, A., Otzen, D.E., Linse, S. & Li, J.-Y. The Bacterial Amyloids Phenol Soluble Modulins from *Staphylococcus aureus* Catalyze Alpha-Synuclein Aggregation. *Int. J. Mol. Sci.* 22, 11594. (2021). 10.3390/ijms222111594
- IV. Reimer, L., **Haikal, C.**, Gram, H., Ruesink, H., Baun, A., Gewering, T., Moeller, A., Li, J. Y & Henning Jensen, P. Low dose DMSO treatment induces oligomerization and accelerates aggregation of α -synuclein. *Sci Rep* (Under review)

Published articles not included in this thesis

- I. Torres-Garcia, L., Domingues, J.M.P., Brandi, E., **Haikal, C.**, Brás, I.C., Gerhardt, E., Li, W., Svanbergsson, A., Outeiro, T.F., Gouras, G.K. & Li, J. Y. Monitoring the interactions between alpha-synuclein and Tau in vitro and in vivo using bimolecular fluorescence complementation. *Sci Rep* (Accepted)
- II. Liu, D., Guo, J. J., Su, J. H., Svanbergsson, A., Yuan, L., **Haikal, C.**, Li, W., Gouras, G.K. & Li, J. Y. Differential seeding and propagating efficiency of α -synuclein strains generated in different conditions. *Translational Neurodegeneration*. 10, 20. (2021). 10.1186/s40035-021-00242-5
- III. Svanbergsson, A., Ek, F., Martinsson, I., Rodo, J., Liu, D., Brandi, E., **Haikal, C.**, Torres-Garcia, L., Li, W., Gouras, G., Olsson, R., Björklund, T. & Li, J.Y. FRET-Based Screening Identifies p38 MAPK and PKC Inhibition as Targets for Prevention of Seeded α -Synuclein Aggregation. *Neurotherapeutics*. (2021). 10.1007/s13311-021-01070-1
- IV. Gou, D.H., Huang, T.T., Li W., Gao, X. D., **Haikal, C.**, Wang, X. H., Song, D. Y., Liang, X., Zhu, L., Tang, Y., Ding, C. & Li, J.Y. Inhibition of copper transporter 1 prevents α -synuclein pathology and alleviates nigrostriatal degeneration in AAV-based mouse model of Parkinson's disease. *Redox Biology*. 38, 101795. (2021). 10.1016/j.redox.2020.101795
- V. Stan, T.L., Soylu-Kucharz, R., Burleigh, S., Prykhodko, O., Cao, L., Franke, N., Sjögren, M., **Haikal, C.**, Hållénus, F. & Björkqvist, M. Increased intestinal permeability and gut dysbiosis in the R6/2 mouse model of Huntington's disease. *Scientific Reports*. 10, 1, 18270. (2020). 10.1038/s41598-020-75229-9
- VI. **Haikal, C.**, Chen, Q. Q. & Li, J. Y. Microbiome changes: an indicator of Parkinson's disease?. *Translational Neurodegeneration*. 8, 38 (2019). 10.1186/s40035-019-0175-7

- VII. Chen, Q. Q., **Haikal, C.**, Li, W. & Li, J. Y. Gut Inflammation in Association With Pathogenesis of Parkinson's Disease. *Frontiers in Molecular Neuroscience*. 12, 218. (2019). 10.3389/fnmol.2019.00218
- VIII. Wu, J-Z., Ardah, M., **Haikal, C.**, Svanbergsson, A., Diepenbroek, M., Vaikath, N. N., Li, W., Wang, Z-Y., Outeiro, T. F., El-Agnaf, O. M. & Li, J. Y. Dihydromyricetin and Salvianolic acid B inhibit alpha-synuclein aggregation and enhance chaperone-mediated autophagy. *Translational Neurodegeneration*. 8, 18. (2019). 10.1186/s40035-019-0159-7
- IX. Zhong, C. B., Chen Q. Q., **Haikal, C.**, Li, W., Svanbergsson, A., Diepenbroek, M. & Li, J. Y. Age-Dependent Alpha-Synuclein Accumulation and Phosphorylation in the Enteric Nervous System in a Transgenic Mouse Model of Parkinson's Disease. *Neurosci. Bull.* 33, 483–492 (2017). 10.1007/s12264-017-0179-1
- X. Valind, A., **Haikal, C.**, Klasson, M. E. K., Johansson, M. C., Gullander, J., Soller, M., Baldetorp, B. & Gisselsson, D. The Fetal Thymus Has a Unique Genomic Copy Number Profile Resulting from T Cell Receptor Gene Rearrangement. *Sci Rep.* 6, 23500 (2016). 10.1038/srep23500

Popular science summary

There is a group of diseases called synucleinopathies, examples of which are Parkinson's disease, dementia with Lewy bodies, and multiple system atrophy. While all humans, and many animals express a protein called alpha-synuclein, in these diseases it folds incorrectly, similarly to what happens with prion proteins in mad cow disease. Even though these diseases are likely caused by the misfolding of alpha-synuclein, they have different symptoms. When we looked at the brains of patients with the different diseases, we found that in Parkinson's disease we more often see a shorter version of alpha-synuclein than in the other synucleinopathies.

While all these diseases are known to affect the brain, recently, attention has also been given to other symptoms that patients often experience many years before they are diagnosed. One such symptom is constipation. We used a mouse model of synucleinopathies and could see these mice developed constipation and accumulated misfolded alpha-synuclein in the neurons of the colon before they started showing other symptoms.

Since these diseases are only inherited in rare cases, we think the trigger that causes alpha-synuclein to misfold is environmental. The bacterial composition in the intestine differs between synucleinopathy patients and healthy controls. We therefore tested different bacterial proteins and found that proteins called phenol soluble modulins, which are produced by *Staphylococcus aureus*, cause alpha synuclein to misfold much quicker than it did on its own. We then infected mice with the bacteria and saw that alpha-synuclein accumulated at the site of the infection. We know from previous studies that misfolded alpha-synuclein can travel from peripheral tissues to the brain and so we plan on testing whether these skin infections can cause alpha-synuclein to accumulate in the brain.

We used a compound called DMSO to dissolve the bacterial proteins and we were curious whether it had an effect on our results. We did observe that in the presence of other factors that could trigger alpha-synuclein to misfold, DMSO accelerated this process. However, when we tube-fed mice with it for 2 weeks, we saw no alpha-synuclein accumulation. This points to DMSO having a synergistic effect on alpha-synuclein misfolding and accumulation: if triggers are there, DMSO will enhance them. With this new knowledge, we hope to better inform the design of therapies and preventative measures for these synucleinopathies.

Populärvetenskaplig sammanfattning

Parkinsons sjukdom är ett exempel på en synukleinopati. Synukleinopatier är en grupp sjukdomar som tros orsakas av proteinet alfa-synuklein. Alfa-synuklein förekommer hos alla, men felvecklas i synukleinopatier. Bland synukleinopatierna finns även sjukdomarna Lewykroppsdemens och multipel systematrofi. Då alfa-synuklein tros orsaka alla dessa sjukdomar, med olika symtom, spekuleras det att alfa-synuklein skulle kunna felvecklas på fler än ett sätt. När vi undersökt hjärnor från patienter med olika typer av synukleinopatier, har vi sett att alfa-synuklein oftare förekommer som en kortare variant i Parkinsons sjukdom än i multipel systematrofi. Detta kan ha en innebörd för hur vi bör utforma terapier för de olika sjukdomarna: det som fungerar för en kanske inte gör det för den andra.

Trots att dessa sjukdomar kännetecknas av hjärnpatologi, har många patienter rapporterat andra symtom, så som mag-och-tarm rubbningar, flera år innan de får diagnosen synukleinopati. När vi har undersökt genetiskt modifierade möss, som får synukleinopati, kan vi se att dessa lider av förstoppning och att alfa-synuklein felvecklas och samlas i tarmens nerver också!

Patienter med synukleinopati har visats ha en annorlunda bakteriell sammansättning i tarmen jämfört med icke-patienter. Detta är spännande då vi vet att vissa bakterier kan utsöndra amyloida protein: protein som vecklas på ett liknande sätt som alfa-synuklein. En sådan bakterie är den vanligt förekommande *Staphylococcus aureus* som utsöndrar proteiner som heter phenol soluble modulins. Tillsatsen av phenol soluble modulins till alfa-synuklein orsakade en snabb felveckling av alfa-synuklein som dessutom kunde orsaka patologi i celler. Vi infekterade således möss med bakterien och såg att dessa möss fick en ökning av alfa-synuklein vid såret.

Då vi använt oss av en substans som heter DMSO för att lösa upp de bakteriella proteinerna, ville vi undersöka hurvida DMSO i sig kan påverka alfa-synuklein. När vi tillsatte DMSO till alfa-synuklein med andra faktorer som kan orsaka dess felveckling, såg vi en synergistisk effekt: dvs, DMSO kunde påskynda felvecklingen så länge något annat initierade den.

Med kunskapen från detta arbete hoppas vi kunna bidra med en bättre förståelse av komplexiteten i synukleinopatier och orsaken till deras uppkomst. Vi hoppas detta kommer bidra till utvecklingen av nya terapier och preventiva medel i framtiden.

Abbreviations

6-OHDA	6-hydroxydopamine
α -syn	Alpha-synuclein
A β	Amyloid beta
BAC	Bacterial artificial chromosome
BAP	Bacterial amyloid protein
CNS	Central nervous system
DLB	Dementia with Lewy bodies
DLS	Dynamic light scattering
DMSO	Dimethyl sulfoxide
DNAJB6	DnaJ Heat Shock Protein Family (Hsp40) Member B6
EBV	Epstein Barr virus
FPD	Familial Parkinson's disease
GCI	Glial cytoplasmic inclusion
GFP	Green fluorescent protein
GI	Gastrointestinal
Hsp10	Heat shock 10 kDa protein 1
HSV	Human simplex virus
Iba-1	Allograft inflammatory factor 1
IPTG	Isopropyl β -D-1-thiogalactopyranoside
L-DOPA	Levodopa
LB	Lewy body
LN	Lewy neurite
LRRK2	Leucine rich repeat kinase 2
MPTP	1-methyl-4-phenyl-1,2,3,6-tetrahydropyridine

MRSA	Methicillin resistant <i>Staphylococcus aureus</i>
MS	Multiple sclerosis
MSA	Multiple system atrophy
NAC	Non-amyloid beta component
NET	Neutrophil extracellular trap
nNOS	Neuronal nitric oxide synthase
p-syn	Phosphorylated alpha-synuclein
PBS	Phosphate buffered saline
PD	Parkinson's disease
PINK1	PTEN-induced kinase 1
pK	Proteinase K
PNS	Peripheral nervous system
PSM α	Phenol soluble modulins, alpha subtype
RBD	REM sleep behavior disorder
REM	Rapid eye movement
SDS	Sodium dodecyl sulfate
SNARE	Soluble N-ethylmaleimide sensitive factor attachment protein
TEM	Transmission electron microscopy
TH	Tyrosine hydroxylase
ThT	Thioflavin T
VIP	Vasoactive intestinal peptide

Introduction

Parkinson's disease (PD), dementia with Lewy bodies (DLB), and multiple system atrophy (MSA) are a group of neurodegenerative diseases collectively termed synucleinopathies (1). PD was first described in 1817 as a shaking palsy (2) and is characterized by its 3 cardinal motor symptoms: rigidity, bradykinesia, and resting tremor. These symptoms arise as a result of the loss of dopaminergic innervation in the basal ganglia characteristic for PD. In recent years, other non-motor symptoms have also been described for PD: REM sleep behavior disorder (RBD) (3), delayed gastric emptying, constipation, pain, depression, and loss of olfaction. These non-motor symptoms often arise many years prior to diagnosis. While cognitive impairment does occur in PD, it often does so at advanced stages of the disease. In DLB, however, the cognitive decline is the main symptom and is required for diagnosis. It is a dementia characterized by visual hallucinations, REM sleep disturbances and some parkinsonism. Prodromal symptoms of DLB are similar to those of PD: RBD, gastrointestinal (GI) disturbances, hyposmia, depression and anxiety. Because frontal brain structures are often affected prior to the hippocampus, memory impairment usually occurs at later stages of the disease compared with other dementias such as Alzheimer's disease. MSA, on the other hand, has a strong autonomic dysfunction component, which is not as pronounced in the two other diseases. It can either be of the parkinsonian subtype with clear involvement of the striatonigral pathway, or of the cerebellar dysfunction subtype with a greater involvement of the olivopontocerebellar pathway. The prognosis of MSA is worse than for PD or DLB and its symptoms and progression are more severe. Common for the diseases are their often idiopathic nature and the accumulation of alpha-synuclein (α -syn) into insoluble aggregates; in PD and DLB into Lewy bodies (LBs) and Lewy neurites (LNs) found in neurons and in MSA in glial cytoplasmic inclusions (GCIs) affecting oligodendrocytes (Figure 1).

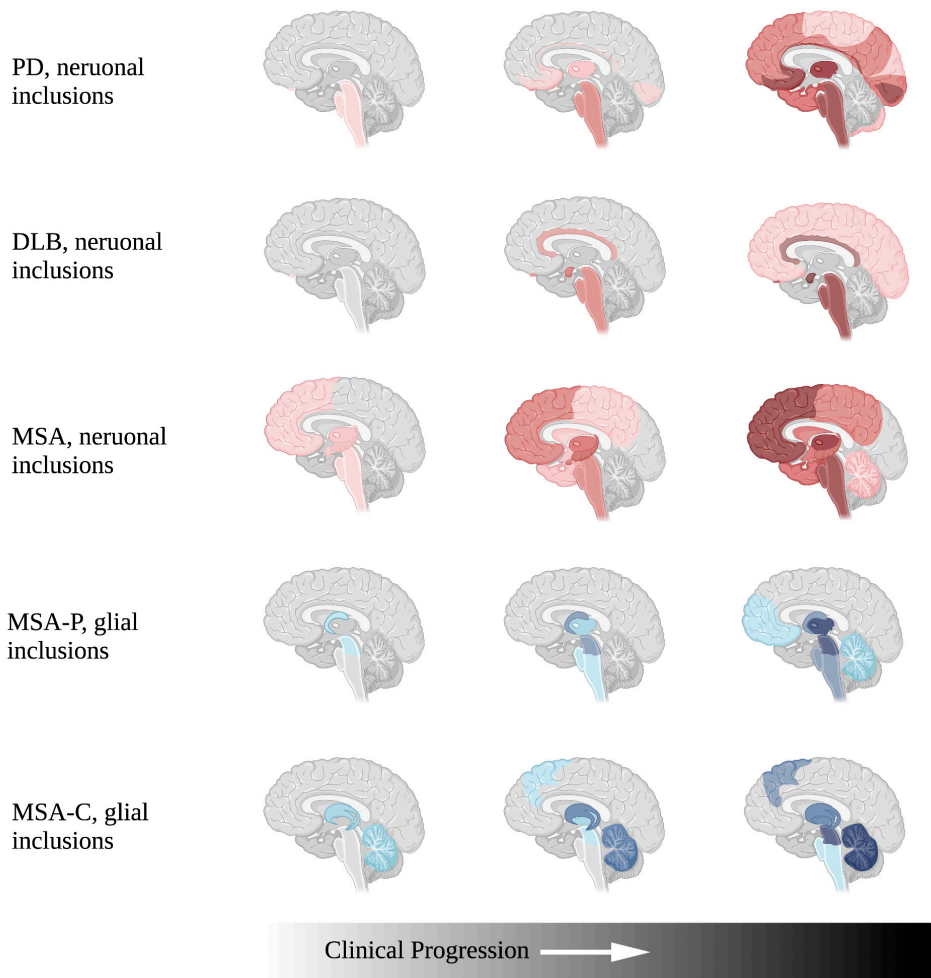


Figure 1. Schematic depiction of spatio-temporal α -syn accumulation in neurons and oligodendrocytes in different synucleinopathies. Diagram made with Biorender based on works characterizing PD (4, 5), DLB (6-8) and MSA (9).

Alpha-synuclein

Discovery of alpha-synuclein

α -Syn was first identified in 1988 in *Torpedo californica*. A homolog in the rat brain was also described (10). A few years later, α -syn was identified as the main protein

of the non-amyloid beta ($A\beta$) component (NAC) of amyloid plaques from Alzheimer's disease patients (11). A 'mutation' in the SNCA gene, which encodes α -syn, resulting in the substitution of alanine to threonine at residue 53 in the protein was identified in a family with familial Parkinson's disease (FPD) (12). Not long after, α -syn was identified as the main proteinaceous component of LBs, LNs (13), and GCIs (14, 15). Polymorphisms in the SNCA gene have also been implicated in MSA (16). Duplications and triplications of the SNCA gene have been linked to FPD, further cementing α -syn's causative role in the disease. Interestingly, even though patients with both duplications and triplications of the SNCA gene develop GCI-like pathology, only patients with triplications present with MSA-like symptoms (17). As α -syn is expressed in neurons to a greater extent than oligodendrocytes, a duplication event in its gene would be expected to affect neurons to a greater extent, in agreement with a dose-dependence for developing pathology. The high penetrance of disease in patients with mutations in the SNCA gene has prompted the intense study of α -syn.

The synucleins

The synuclein family is composed of alpha, beta, and gamma isoforms encoded by different genes. The synucleins have been suggested to be vertebrate-specific, and the diversification of SNCA is suggested to have occurred at the root of the sarcopterygian's lineage. The N-terminal region of α -syn was found to be the most highly conserved with only one substitution (the T53A) occurring at the branching of catarrhines, as opposed to the NAC region and C-terminus, where several substitutions throughout evolution could be identified (18). This points to the N-terminus playing a critical role, further underlining the importance of the FPD variants of SNCA all having amino acid substitutions in the N-terminus.

Alpha-synuclein's physiological role

The N-terminus of α -syn contains seven imperfect KTKEGV repeat motifs, similar to those of apolipoproteins (19-21). It is lipophilic and has been shown to assume an alpha-helical structure upon interaction with lipids, then selectively binding to curved, negatively charged lipid bilayers. Its affinity to membranes is thought to underlie its participation in vesicle trafficking and dilation of the exocytotic fusion pore (22). It is involved in neurotransmission at synapses and interacts with the SNARE complex (23). Recently, α -syn has been shown to exhibit positive cooperativity in lipid-binding: when binding to membranes, α -syn preferentially binds to vesicles where other α -syn proteins are already bound and does not distribute evenly across the vesicles (24). This cooperativity phenomenon could be fundamental to α -syn's role in membrane remodeling and vesicle trafficking and

docking. Triple synuclein knockout mice exhibit intact brain structure but decreased synapse formation (25). The SNCA amino acid substitutions linked to monogenic presentations of synucleinopathies are A30P (26), E46K (27), H50Q (28), G51D (29), A53T (30), A53E (31), and A53V (32). These mutations all fall around the third and fourth motif repeats (Figure 2) and unsurprisingly affect α -syn's lipid affinity, although investigations into this have yielded contradictory results. (33, 34). It has been suggested that the amino acid substitutions result in a loss of selectivity for curved membranes (35). Aberrant binding to vesicles could underlie organelle dysfunction seen in synucleinopathies. α -syn has been shown to bind to mitochondrial cardiolipin, resulting in the loss of integrity of the mitochondrial membrane (36), and overexpression of SNCA results in fragmentation of mitochondria (37). Mitochondrial dysfunction is well described in synucleinopathies and can both be caused by and cause α -syn accumulation (38). There are other positive-feedback loops relating to α -syn and altered organelle function: disruptions to the ubiquitin-proteasome system (39), lysosomal dysfunction (40), and decreased autophagy all contribute to the accumulation of α -syn, which in turn can aggravate the dysfunctions.

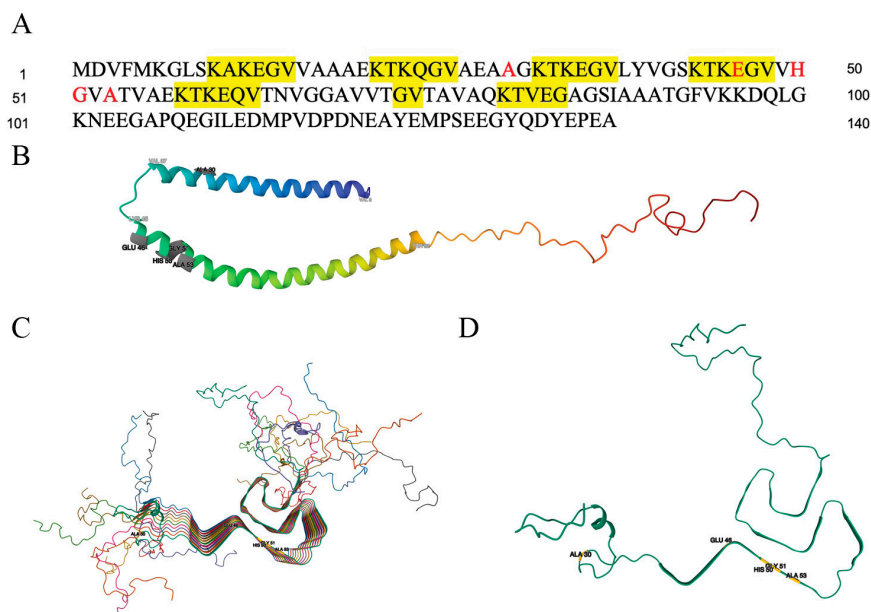


Figure 2. α -Syn structure. A. The amino acid sequence of α -syn with the different KTKEGV motifs highlighted in yellow and residues identified in FPD marked in red. B. Upon association with micelles, α -syn assumes a conformation with α -helical domains within residues 3-37 and 45-92 (residues marked in light grey) as previously described (41). FPD associated residues are located within both helices and are marked in dark grey. C. Atomic resolution structure of α -syn fibrils showing typical amyloid cross- β sheet structure as described (42). D. Singular chain from the fibril. FPD associated residues are marked in yellow and all except alanine 30 appear within the β -sheet. B, C, and D were created using RCSB PDB Mol* viewer (43) with IDs: 1XQ8 (B) and 2N0A (C,D).

Pathology

Amyloidosis

To better understand its physiological role, α -syn's structure has been studied. α -Syn is often described as an intrinsically disordered monomer at physiological conditions or, controversially, as a tetramer (44). While the native folding of a protein is determined by its amino acid sequence, several proteins are known to adopt a different conformation; these proteins can all adopt a similarly β -sheet rich structure favoring multimerization into fibrils and are termed amyloid proteins. Much of the α -syn in LBs, LNs, and GCIs is in fibrillar form. Homogeneous primary nucleation whereby monomers self-assemble into aggregates is slow and requires overcoming a high energy barrier. Initial seeds can also be formed by heterogeneous primary nucleation, wherein a foreign object catalyzes the aggregation of α -syn. This is thought to be the primary means of seed formation *in vivo*. Once an initial seed has been formed, however, the aggregate mass can rapidly be amplified either by elongation wherein monomers add onto fibril ends forming larger fibrils or by secondary nucleation wherein the surfaces of the seeds catalyze the formation of new aggregates (Figure 3) (45). In cell-free conditions, buffer conditions and the seed-to-monomer ratio can modify the relative contribution of either process to the aggregate mass amplification. Lowering pH and salt screening reduce electrostatic repulsion between monomers, favoring secondary nucleation. While elongation faithfully propagates the parent seed conformation, secondary nucleation can give rise to fibrils with a different conformation. Interestingly, in 2013, an article described the formation of structurally different polymorphs of α -syn fibrils generated from the same protein monomer under different buffer conditions (46). Since, several articles have described protocols for generating α -syn fibrils with particular structural properties by modulating the buffer concentrations and pH, salt concentrations and the use (or lack thereof) of agitation and other nucleating factors such as polystyrene. Interestingly, these different polymorphs of fibrils have different propensities for inducing elongation or secondary nucleation: some fibrils can be used at lower seed concentrations and still favor elongation. However, when starting seed concentration is very low and secondary nucleation is favored, the buffer conditions determine the polymorph of fibrils generated (47). The different FPD-associated variants of α -syn exhibit different propensities for aggregation under agitation conditions (33). Additionally, it seems different microscopic steps are affected by these amino acid substitutions: the H50Q and G51D variants exhibit minimal rates of secondary nucleation compared to the other variants (34). Interestingly, the G51D variant is not seeded by fibrils of wildtype α -syn.

A prion-like hypothesis of alpha-synuclein pathology

α -Syn's capability to form different polymorphic fibrils and its involvement in diseases with distinct phenotypes is reminiscent of prion proteins. Different prion strains from the same prion protein, have been described with distinct proteolytic cleavage patterns, cell infectivity profiles, pathology spreading patterns, and disease phenotypes. Interestingly, the hosts' gene dosage and prion protein expression level can determine which strain is propagated when animals are infected with the same starting material (48). A key aspect of prions' infectious nature is their ability to propagate between cells and tissue types and template the native cellular prion protein into the insoluble aggregates in prion plaques. In 2008, two studies identified Lewy pathology in transplanted fetal dopaminergic neurons in PD patients (49, 50). The young age of the transplanted neurons suggested their α -syn pathology was not endogenous and so a hypothesis of host to graft pathology spread was proposed. A few years prior, Braak had examined Lewy pathology in different brain regions of patients with PD. In his study, he proposed a staging profile wherein Lewy pathology temporally spread from the brain stem up to the midbrain and cortex. In this landmark study, Braak identified Lewy pathology in the dorsal motor nucleus of the vagus and the olfactory bulb at the very earliest stages of the disease. Thus, he proposed that Lewy pathology could be initiated in the periphery wherefrom it would propagate retrogradely (51). Subsequent studies have identified phosphorylated α -syn (p-syn) in the GI tract of prodromal PD patients (52) and retrospective studies have shown that truncal vagotomies decrease the risk of developing PD (53). Since then, a number of studies have indeed shown that aggregated α -syn is capable of propagating from the duodenal wall (54), intestinal lumen (55) and olfactory bulb (56-58) to the CNS. Thus the heterogeneity of synucleinopathies could be attributed to different polymorphs of α -syn or different tissue origins and subsequent spreading routes. In a study wherein aggregated α -syn was purified from PD and MSA patients, MSA-derived α -syn gave rise to a more aggressive phenotype and a distinct spreading pattern. However, when PD-derived α -syn was added onto oligodendrocyte cultures, the protein underwent processing resulting in seeds reminiscent of the MSA-derived α -syn. The intracellular milieu was thus deemed responsible for forming the different polymorphs (59). This is in agreement with a model of secondary nucleation dominating the *in vivo* aggregate mass amplification.

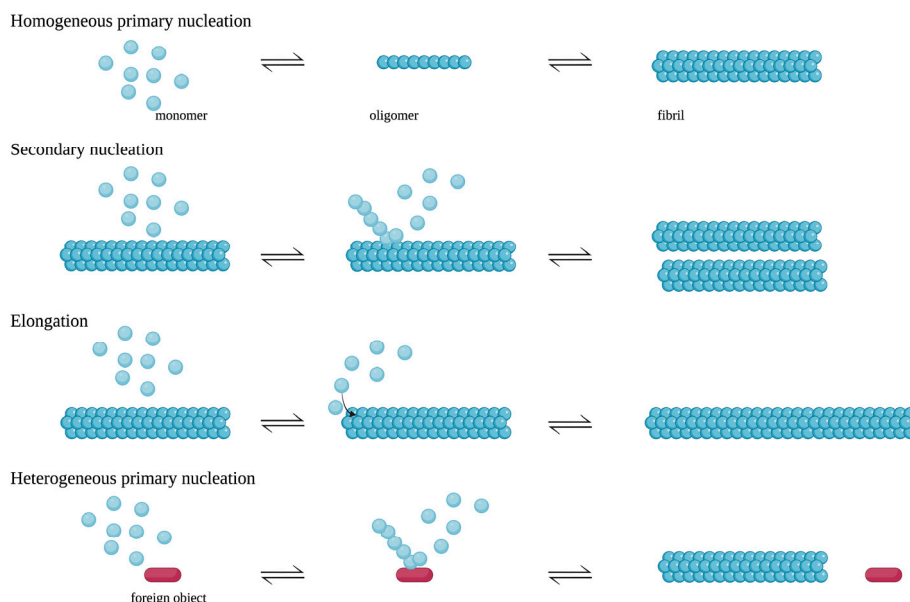


Figure 3. Schematic depiction of aggregation processes. An aggregation prone protein in bulk monomer solution can aggregate through homogeneous primary nucleation. Once fibrils have formed, aggregate mass can be amplified by secondary nucleation, wherein aggregation of the monomer is catalyzed by the surface of the fibril, or by elongation wherein monomers add onto the fibril ends. In the presence of foreign objects, such as polystyrene nanoparticles, lipids, or other proteins, heterogeneous primary nucleation, wherein the foreign object's surface catalyzes the aggregation of the monomer solution can form the initial seeds.

Environmental triggers of alpha-synuclein pathology

This raises the question: if indeed α -syn can propagate from the periphery, what induces the formation of the initial seed(s)? In cases of gene duplications or triplications, a higher concentration of α -syn could trigger its aggregation if the concentration reaches above the solubility. However, considering the low prevalence of heritable forms of synucleinopathy, environmental causes have been speculated to underlie the different diseases. Organopesticides (60), and the toxin MPTP (61) have been identified to cause α -syn aggregation and dopaminergic neuronal loss. These, however, do not account for all the idiopathic cases of synucleinopathy, so the focus has instead shifted to other environmental aspects. In recent years, much attention has been given to the microbiome. This is in part due to non-motor symptoms of PD that can arise decades prior to motor symptom onset and diagnosis and often involve both the GI tract. Delayed gastric emptying and constipation are such symptoms. A correlation between inflammatory bowel disease and PD has been shown (62) and common mutations in the LRRK2 gene underlying

both diseases have been identified (63). Dysbiosis, a change to the microbiome, which has long been associated with IBD, has been studied in PD patients. Consistently, PD patients show significant beta diversity compared to healthy controls, i.e., significant community differences between the groups. However, when looking at particular bacterial species or genera, the results are often contradictory, perhaps because methodology differs substantially and the low number of participants (64). While studies examining microbiome changes in DLB and MSA patients are lacking, this is not indicative of a lack of dysbiosis. Another interesting observation has come from transgenic animals, overexpressing α -syn, which tend to develop synucleinopathy: when kept in germ-free conditions, they develop fewer plaques. In 2016, a study further examined the relationship between the microbiome and α -syn pathology using M83 mice, which overexpress the human A53T variant of α -syn. When kept under germ-free conditions, these mice developed fewer symptoms and pathology in accordance with previous studies. The most interesting observation, however, came from transplanting human fecal matter, either from PD patients or healthy controls, into these mice. Mice that had received material from PD patients developed more severe symptoms than those that received from healthy controls (65). This points to the microbiome playing a causative role.

Microbes, the immune system, and neurodegeneration

In 1991, researchers at UC Davis described how infecting mice with sublethal doses of the common soil bacterium, *Nocardia Asteroides* (since renamed to *Nocardia cyriacigeorgica*), known to cause pulmonary disease, led to bacterial localization to the pons. Many of the mice subsequently developed parkinsonian-like symptoms such as a resting tremor and responsiveness to L-DOPA treatment (66). In 2009, another study identified a metabolite by another common soil bacterium, *Streptomyces venezuelae*, as neurodegenerative with dopaminergic neurons particularly affected (67). In 2016, researchers identified the Curli proteins CsgC and CsgE, which inhibit fibrillation of the amyloid CsgA, as modulators of α -syn aggregation *in vitro*: CsgE accelerated α -syn aggregation whereas CsgC inhibited it (68). A follow-up study showed that animals colonized by Curli-producing *Escherichia coli* developed astrogliosis, microgliosis, and increased α -syn aggregate deposits (69). This is reminiscent of another human amyloid protein: amyloid beta ($A\beta$) has been shown to rapidly aggregate in response to infection with *Chlamydia pneumoniae* (70) and Herpes Simplex Virus (HSV) (71) *in vivo*, and upon binding to the viral corona of HSV as well as the respiratory syncytial virus *in vitro* (72). A role in immunity for both α -syn and $A\beta$ has thus been proposed.

For α -syn, this role is strengthened by several observations. Addition of monomeric α -syn solutions to bacterial cultures of *E. coli*, *Staphylococcus aureus*, *Pseudomonas. aeruginosa*, and *Staphylococcus epidermidis* resulted in an inhibition

of bacterial growth already at 0.2 μ M α -syn concentration. Similarly, adding α -syn to cultures of *Candida albicans* and several other fungi inhibited culture growth (73). α -Syn knockout mice displayed poorer immune responses and survival rates when infected with West Nile Virus, Venezuelan Equine Encephalitis Virus (74), Reovirus T3D and *Salmonella typhimurium* (75). A relevant finding is a neuronal involvement in the immune response to *S. aureus* (76), *Streptococcus. pyogenes* (77) and *C. albicans* (78), where the pathogen's activation of sensory neurons can either aid or impede the immune response against its subsequent clearance. Similarly, A β has been shown to inhibit the growth of *E. coli*, *S. aureus*, *C. albicans* and several other microbes (79). Also, A β null mice exhibited poorer survival rates when infected with *S. typhimurium* (80). In contrast, overexpression of A β -precursor protein resulted in increased survival compared to wildtype littermates when mice were infected with HSV-1 (71) or *S. typhimurium* (80). A β was found to mediate pathogen entrapment similarly to already well-described models of antimicrobial-protein-mediated microbial agglutination. These findings are even more interesting as reports have identified *C. pneumoniae* (81), HSV-1 (82, 83), Borrelia species (84), and several different genera of fungi (85-87) in AD brains. Just recently, species of bacteria and fungi have also been identified in PD brains (88). However, even though these studies are striking, several fail to include control patients in their analyses which could help cement the hypothesis that these findings are not artifacts from tissue processing and are specific to the diseased brains. An infection-based model of neurodegenerative disease does not necessarily rely on the finding of microbial species in the brains. This could be an effect of a breakdown of the blood-brain barrier at later stages of the disease. Instead, if infection underlies neurodegenerative diseases, it could very well be a peripheral infection that has long since cleared as aggregated human amyloid proteins have been shown capable of propagating from the PNS to the CNS. A recently published study has shown a causative role of the Epstein Barr virus (EBV) in the pathology of multiple sclerosis (MS) (89). While an association of EBV and MS has long been speculated to exist, findings of EBV in some but not all MS patients has raised doubts to its involvement. However, this longitudinal study, could convincingly show all but one subject who developed MS over the course of the 20-year-long study were infected with EBV prior to any pathological alterations such as elevated serum neurofilament in blood samples. It is as such argued that the latent and persistent EBV colonization reprograms B-cells, perhaps by molecular mimicry, to initiate an autoimmune response to myelin. Similarly, longitudinal studies of commensal microbiome particulates could elucidate causative roles for viruses, bacteria or fungi in the synucleinopathies. Several microbes and pathogens are also known to cause host DNA damage and epigenetic changes, as evidenced by infection-induced tumorigenesis (90). Aberrant methylation of genes relating to the autophagy-lysosomal pathway has been described in PD (91). Interestingly, SNCA knockdown resulted in increased DNA strand breaks which could be attenuated by the

reintroduction of the protein (92). Thus, α -syn could play a role in the host's DNA damage response.

Neuroinflammation

Another argument for the involvement of infection is the well-described inflammation component of neurodegenerative diseases. Brains from patients with synucleinopathies show extensive microgliosis and astrogliosis as well as infiltration of peripheral immune cells. Aggregated α -syn has been shown to activate the immune system, driving inflammation. Inflammation could enhance α -syn aggregation by releasing reactive oxygen species and activating caspase-1, which can cleave α -syn into a more aggregation-prone peptide (93). Many have described a neuroinflammatory profile of microglia in synucleinopathies instead of the homeostatic neuroprotective role in control cases (94). Interestingly, SNCA knockout mice develop immature T lymphocytes, with CD4⁺ cells particularly affected. The few mature CD8⁺ cells that could be identified showed signs of overactivation, and CD4⁺ cells produced IL-2 to a greater extent than CD4⁺ cells isolated from wildtype mice (95). T lymphocytes, specifically CD4⁺ cells, are particularly crucial to α -syn pathology in the toxin (96), overexpression (97), and fibril (98) mouse models. Peripherally, PD patients have also shown signs of altered activation and survival rates of monocytes (99), a decrease in CD4⁺:CD8⁺ ratio (100, 101), and α -syn reactive T cells (102). Also, the vagus nerve is known to play an important role in the neuroimmune axis, through the hypothalamic-pituitary-adrenal axis by its afferents, regulating release of glucocorticoids, through the splenic nerve with its efferents regulating the release of tumor necrosis alpha, as well as through the inflammatory reflex involving both the vagal afferents and efferents and the cholinergic system (103). The microbiome can be implicated here, too, as it can prime the immune system towards specific profiles and responses. The immune system, in turn, can alter the microbiome composition: microRNA released by intestinal epithelial cells can alter gene transcription in bacteria (104, 105). These vicious-cycle positive-feedback loops could underlie the chronic nature of inflammation in neurodegenerative diseases.

Outlook

The presence of chaperones such as hsp70, which, together with its co-chaperones DNAJB1 and hsp110, can disaggregate α -syn (106-108), indicates there might be physiological roles to α -syn aggregation and disaggregation. In yeast cells, heat or other stress conditions give rise to the formation of protein aggregate centers into which misfolded proteins are sequestered by chaperones. Once the stressor is

eliminated, the aggregated proteins are refolded to recover activity. This mechanism preserves energy by protecting the proteins from degradation (109). The aggregation of α -syn could thus be an adaptive strategy towards cellular stress, an entrapment strategy against microbes, or simply a misfolding event that burdens the host cell. The complex mechanisms underlying the synucleinopathies as well as the progressed state at which they are diagnosed complicate the development of preventative and therapeutic strategies. Thus far, therapies have focused on symptomatic relief by replacing the dopamine deficit caused by the degeneration of dopaminergic neurons in PD, either through L-DOPA treatment or cell replacement therapy. Disease-modifying therapies target systems that are not specific to synucleinopathies, such as kinases and mitochondria, or aim to minimize or reverse α -syn aggregation by immunotherapy with anti- α -syn antibodies or small molecule aggregation inhibitors (110). Even though these treatments have shown promising results in preclinical studies, the effects have not translated into clinical settings. This perhaps indicates a need for better preclinical models of the diseases, accounting for peripheral involvement and multi-system dysfunction, as opposed to the models often used, which capture only particular aspects of the diseases. Elucidating the role and mechanism of α -syn aggregation and the development of better models of synucleinopathies could thus redirect therapeutic and preventative strategies for the different synucleinopathies. To do so, we have studied differences in α -syn presentations in different synucleinopathies, employed animal models to study the natural expression patterns of α -syn, and examined the interaction of α -syn with environmental agents.

Aims

In this thesis, we have aimed to answer questions relating to α -syn's presentation in disease and disease models as well as its aggregation in the presence of extrinsic factors. We have thus designed four studies with the following objectives:

- I. Examine distinct α -syn species in different synucleinopathies and brain regions to better understand disease heterogeneity which might guide the design of future immunotherapies
- II. Describe peripheral α -syn expression, particularly in the colon, of a relevant mouse model of synucleinopathy
- III. Investigate the impact of bacterial peptides on α -syn aggregation to understand the potential of an infection-based model of synucleinopathy
- IV. Evaluate the effect of DMSO, a commonly used solvent in α -syn aggregation studies, on α -syn to deter from drawing incorrect conclusions

Summary of key results

Paper I

Full-length human α -syn is composed of 140 amino acids, yet several other forms of the protein have been described. These result from alternative splicing, resulting in a protein lacking residues 41-54 and/or 103-130, and post-translational modifications such as N- and C-terminal truncations, acetylation, nitration, phosphorylation and ubiquitination (111, 112). Different forms of α -syn have been described to have different aggregation propensities and potencies in inducing toxicity *in vitro* and *in vivo* (113, 114). As such, it would not be unexpected that certain α -syn forms localize to aggregates in tissues to a higher extent than others. One study found that while α -syn truncated at residue 119 was equally present in the cytosol and LBs, α -syn phosphorylated at serine 129 was particularly enriched in the insoluble fractions of isolated α -syn from brains of DLB and MSA patients (115). This study, however, primarily used brain homogenates to quantify differences in α -syn species. Differently sized aggregates might also differ in α -syn species composition but examining homogenates would not reveal this. Additionally, this study examined only the cingulate, temporal and frontal gray matter. α -syn pathology is known to affect several cellular processes and also induce neuroinflammation. Inflammation activates caspase-1, which in turn cleaves α -syn (116). A temporal α -syn spread to different areas of the brain could result in a spatial map of different α -syn species. As α -syn is a major component of the deposits observed in all synucleinopathies with different symptomatology and spreading patterns, it wouldn't be unexpected that the protein present in different forms in the various diseases. Therefore, we compared α -syn forms in different brain regions of patients with different synucleinopathies and used a set of antibodies with epitopes ranging from the N-terminus to the C-terminus of α -syn.

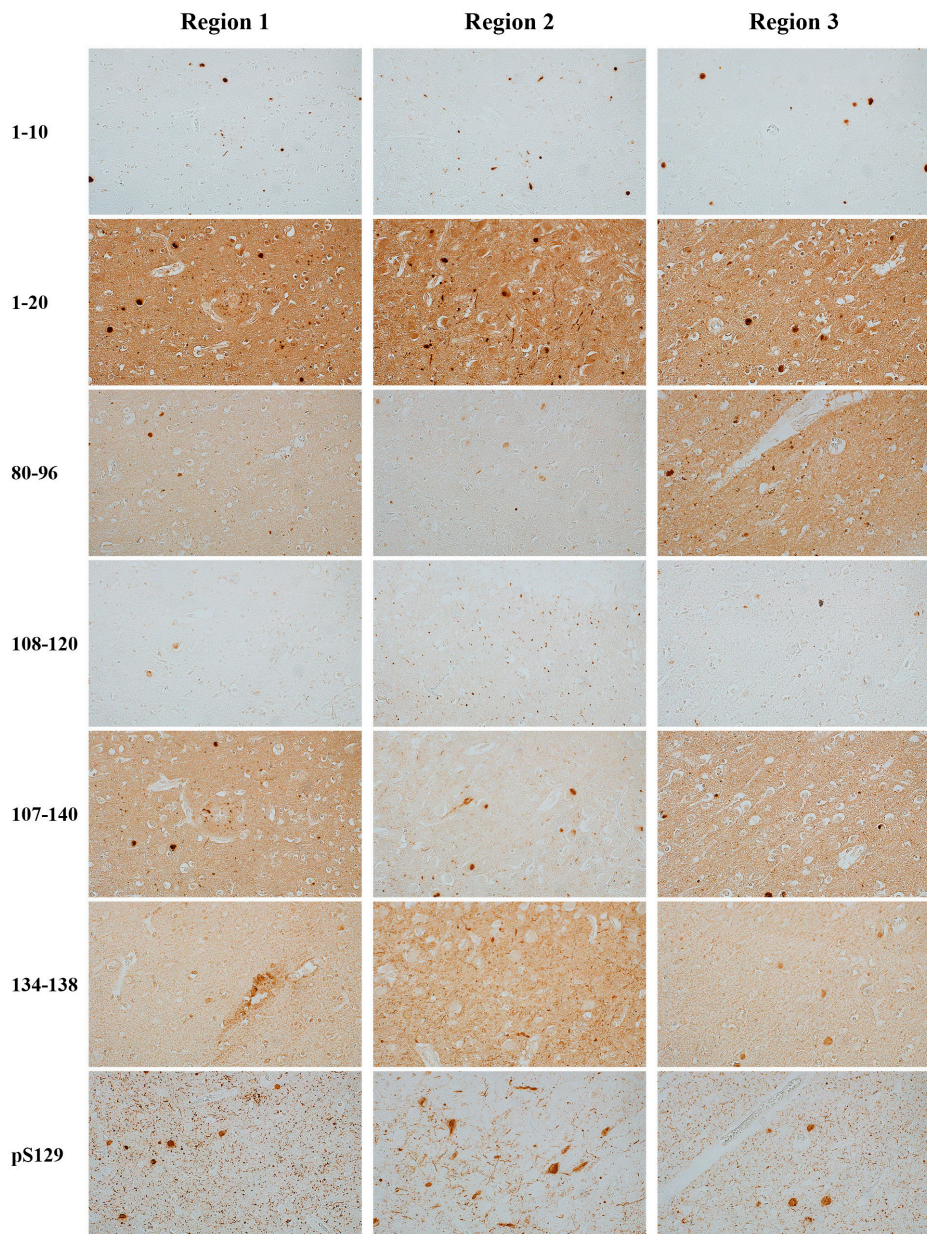


Figure 4. Consecutive hippocampal sections from a patient with DLB stained with antibodies against different epitopes of α -syn. 5 μ m thick consecutive sections of hippocampus were stained by antibodies detecting different epitopes of α -syn as given in the figure and images taken in corresponding areas. Different patterns of LB, LN and nerve terminal staining can be observed for the different antibodies. Scale bar = 20 μ m

Firstly, we examined whether the different antibodies would preferentially identify different forms of α -syn and different pathological hallmarks (Figure 4). Strikingly, the antibody detecting p-syn readily detected structures not identified by any other antibodies. The small aggregates were very numerous and differed from the LBs and LNs detected by the other antibodies. This could indicate a particular conformation of p-syn wherein the other epitopes are hidden. Alternatively, it could indicate the unspecific binding of the antibody to other epitopes. Interestingly, within the same DLB patient, the antibody targeting residues 34-45 detected LBs in the frontal cortex but not the hippocampus. In contrast, in a PD patient, this antibody detected LBs and LNs in the hippocampus but not in the frontal cortex. In both cases, the presence of pathology in both the frontal cortex and hippocampus was verified by other antibodies (Figure 5). Thus, α -syn could be differently processed in different brain regions within the same patient. Whether the seemingly different forms of α -syn affect propagation or are a result of disease progression remains to be determined.

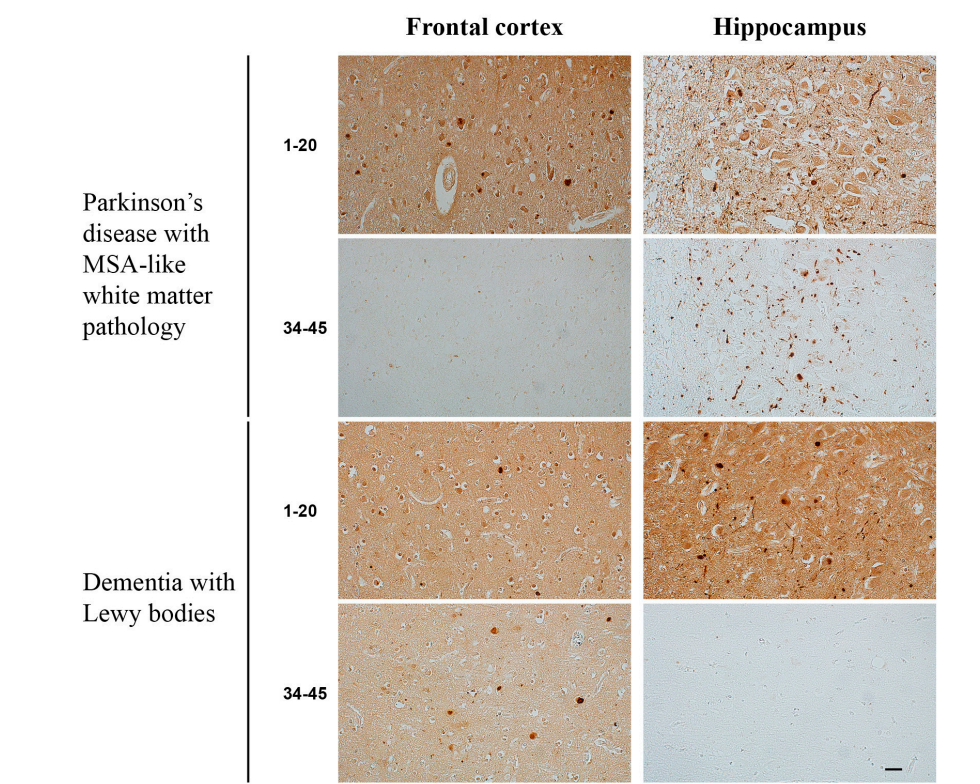


Figure 5. Frontal cortex and hippocampus from patients with PD and DLB stained with 2 antibodies against different epitopes of α -syn. 5 μ m thick consecutive sections of frontal cortex and hippocampus from patients with different synucleinopathies were stained by 2 antibodies detecting epitopes 1-20 and 34-45 of α -syn. Scale bar = 20 μ m

DIAGNOSIS	AGE	SEX	RACE	PMI (H)	BRAIN REGION	α-SYN EPIOTOPE														
						1-20			80-96			134-138			pS129					
						LB	LN	NT	LB	LN	NT	LB	LN	NT	LB	LN	NT			
PD	84	Female	White	23.5	Hippocampus	+	+	++	++	-	+	-	+	-	+	-	+	-		
					Substantia nigra	++	++	-	++	-	+	+	++	+	++	+	-			
					Amygdala	+	+	++	+	+	+++	-	-	-	++	+	-			
					Putamen	+	+	+	+	+/	-	-	-	+	+	+	+			
					Cortex	+/	+/	+	+/	+/	+++	-	-	-	-	-	-			
PD	82	Female	White	8	Cerebellum	-	-	+	+/	+/	+	-	-	-	-	-	-			
					Hippocampus	+	+	++	-	+	+	-	+	-	+/	-	-			
					Substantia nigra	++	+	-	+++	+++	+	-	+	-	+/	-	-			
					Amygdala	++	++	+	++	++	+++	-	+	-	+/	-	-			
					Putamen	+	+	++	+	+	+++	-	++	-	+/	-	-			
PD	84	Male	White	4	Cortex	+/	+/	++	-	-	+++	-	-	-	+/	+/	-			
					Cerebellum	-	-	++	-	-	+++	-	-	-	+/	-	-			
					Hippocampus	+/	+/	++	+/	-	+++	-	+/	-	+/	-	-			
					Substantia nigra	+++	++	-	++	++	++	++	++	-	+++	+	-			
					Amygdala	+	+	++	+	+	+++	++	++	-	+	+	-			
MSA	69	Female	Asian	4.5	Putamen	+/	+/	-	+/	-	+	-	+	++	+	+/	-			
					Cortex	+/	+/	++	+/	-	+++	-	-	++	+	+/	++			
					Cerebellum	+/	+/	++	+/	-	++	-	-	++	+	+/	++			
					Hippocampus	+	+	++	++	-	+++	++	-	++	+/	+/	+			
					Substantia nigra	++	+	+	++++	+	++	++	++	+/	++	++	-			
MSA	69	Male	White	3	Amygdala	+	+	++	+	-	+++	++	+/	++	++	+	-			
					Putamen	++	+/	-	++++	+	++	++	++	+/	++	++	+			
					Cortex	+	+/	++	++++	+/	++	++++	+/	+	++	+	-			
					Cerebellum	++	+	++	++++	-	+++	++++	+/	+	+++	+	-			
					Hippocampus	+++	++	+	++++	+	++	++++	+/	++	+++	+++	+			
MSA	69	Male	White	3	Substantia nigra	+++	++	+/	++++	+	++	+++	+	-	++	+	+/			
					Amygdala	++	++	+	++++	+	++	++++	++	++	+	+	-			
					Putamen	+++	++	+	++++	+	++	+++	++	++	+++	++	+			
					Cortex	++	+	++	++	+	++	++	++	+	++	+	-			
					Cerebellum	+	-	++	++	-	++	+	+	+	+	-	-			

Table 1. Quantification of detected pathology in different brain regions of patients with different synucleinopathies using antibodies against different epitopes of α-syn. LB* = Lewy bodies. LN= Lewy neurites. NT = Nerve terminals. * For the patients with MSA, LB instead refers to glial cytoplasmic inclusions.

To compare α -syn form differences between synucleinopathies, the hippocampus, substantia nigra, amygdala, putamen, cortex (Brodmann 9/46), and cerebellum from patients with PD, DLBD, MSA and control patients were compared. The staining patterns revealed by antibodies against residues 1-20, 80-96 and 134-138 as well as p-syn were subjectively quantified (Table 1). For PD patients, but not MSA patients, the antibody targeting residues 134-138 revealed less α -syn pathology than other antibodies. This indicates α -syn is C-terminally truncated or has a conformation wherein the C-terminus is hidden to a greater extent in PD than MSA. This is interesting because neuroinflammation is thought to play a more prominent role in MSA than PD. So, caspase-1, implicated in α -syn truncation, would be expected to be particularly active in MSA. These findings could indicate that caspase-1 and neuroinflammation are not the main drivers of α -syn C-terminal truncation.

Finally, these samples were double-labeled with antibodies targeting residues 80-96 and 134-138. In PD patients, we could detect LBs stained for residues 80-96 but not 134-138, indicating the presence of truncated α -syn in the LBs. In contrast, larger GCIs and LBs were always stained for both antibodies in the MSA patient examined. Instead, smaller aggregates would occasionally stain solely for one antibody but not the other (Figure 6). This could indicate that part of the maturation of LBs and GCIs in MSA involves the recruitment of different forms of α -syn or that aggregates composed of C-terminally truncated α -syn do not form aggregates past a certain size in MSA.

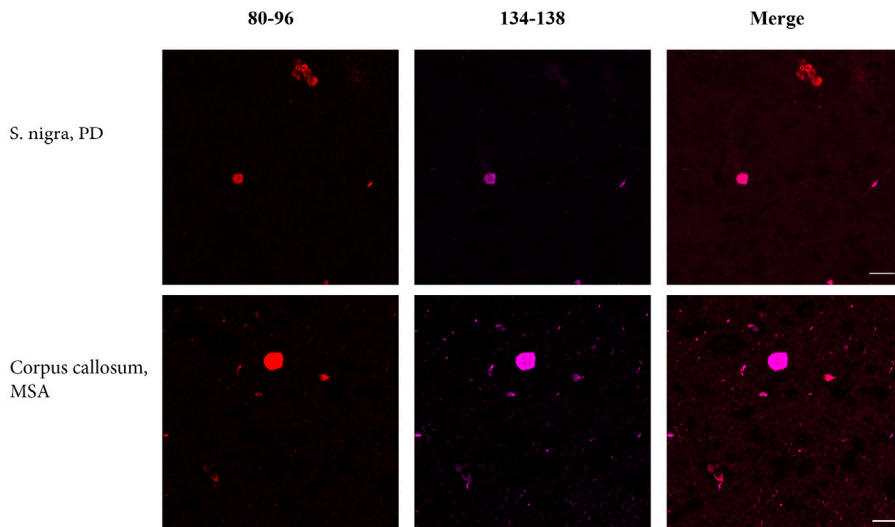


Figure 6. Double-labelling of substantia nigra from PD patient and corpus callosum from MSA patient. 5 μ m thick paraffin sections were labeled with antibodies targeting epitopes 80-96 and 134-138 of α -syn. Maximum intensity projections from z-stacks are shown. Scale bar = 20 μ m.

Paper II

In modeling PD, most have strived to recapitulate the two main facets of the disease: dopaminergic neuron loss and α -syn accumulation. Toxin-induced models, most commonly those utilizing MPTP or 6-OHDA, rapidly induce dopaminergic neuron loss and subsequently, movement-related symptoms. However, they do not result in a satisfactory accumulation of α -syn. Animals treated with α -syn preformed fibrils can display many PD-associated pathologies: α -syn aggregate formation, neuroinflammation, and sometimes dopaminergic neuron loss (117). Yet these are heavily dependent on the fibrils used as well as accuracy and route of administration. Also, interestingly, this model displays first an increase in α -syn aggregate formation with α -syn burden subsequently decreasing, perhaps indicating this model as suboptimal for the study of the chronic nature of the disease (59). While sometimes performed on wildtype mice, these models are often performed in conjunction with vector-induced α -syn overexpression in certain cell populations. Vector-based models of α -syn overexpression are also widely used on their own. However, they are perhaps most suited to studying the effects of α -syn pathology locally instead of modeling a complex, multi-organ disorder.

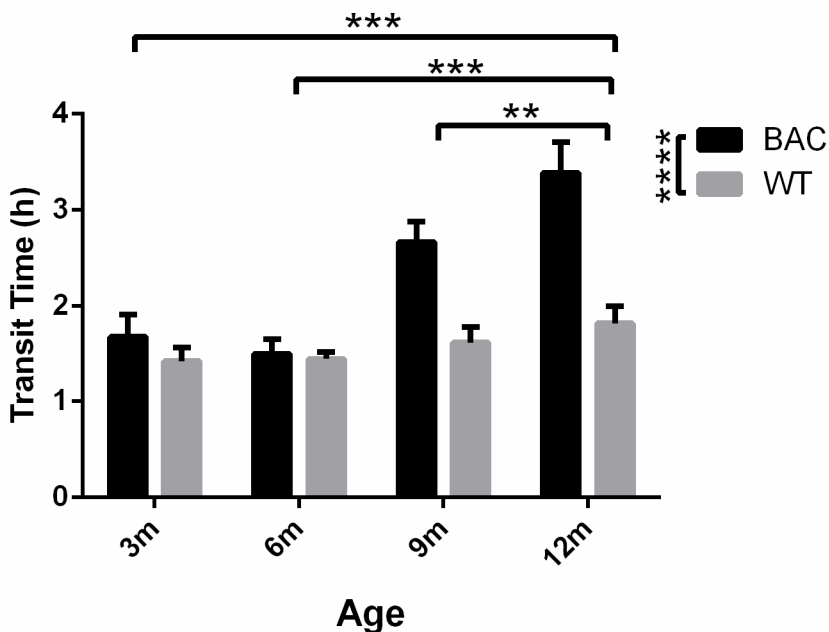


Figure 7. Transgenic mice overexpressing full length wildtype human α -syn develop constipation. C57bl/6 and transgenic BAC-SNCA-GFP mice were tube-fed with carmine and intestinal transit time measured. The transgenic mice displayed delayed transit time from 9 months of age. $n=3$.

Finally, transgenic models have been used to model the complexity of the disease with manipulation to genes implicated in PD by genome-wide association studies. PINK1 knockout animals show mitochondrial dysfunction, and LRRK2 mutant models show decreased autophagy and both models show a progressive dopaminergic neuron loss. Still, most commonly, models of α -syn overexpression are employed. Here, the SNCA variant and promoter choice are vital in determining the pathological outcomes (118). Models using the A53T variant often show aggressive pathology with early disease onset and rapid disease progression. The use of the Thy-1 promoter limits expression to neuronal cells, whereas the use of the prion promoter results in more widespread pathology. To more accurately model α -syn pathology in cell populations and tissues where it would normally be expressed, we use a mouse model expressing the human wildtype α -syn protein (fused to green fluorescent protein (GFP)) under the control of the mouse's endogenous SNCA promoter. In this mouse model, hereto forth called BAC-SNCA-GFP, we see a progressive accumulation and phosphorylation of α -syn, first in the brainstem and olfactory bulb, and in the cortex towards later stages. This mouse model also displays behavioral deficits starting at nine months of age (119).

As Braak's hypothesis, and subsequent studies, have pointed to the GI tract as an area of interest in PD pathology, we wanted to evaluate intestinal pathology in this mouse model. The transgenic mice displayed delayed stool transit time compared to their wildtype counterparts at nine months of age. The wildtype mice showed a moderate increase in stool transit time with age (Figure 7). While GI disturbances in PD are thought of as a consequence of dopaminergic neuron loss, this mouse model shows a moderate decrease in dopaminergic innervation, only at older age. To evaluate whether this constipation was correlated to enteric α -syn pathology, we examined the proximal and distal colons of our transgenic BAC-SNCA-GFP mice at different ages. At three months of age, some GFP signal, indicative of human α -syn expression, could be observed in the nerve fibers. This expression increased with age, becoming more robust in the submucosal and myenteric plexi and around the crypts of Lieberkühn (Figure 8). To evaluate whether this α -syn was phosphorylated, we stained the intestines with an antibody specifically recognizing p-syn. P-syn could be detected in both the proximal and distal colon segments, in the neural fibers in the submucosal and myenteric plexi from six months of age, and again, increased with age (Figure 9). The α -syn colocalized with calretinin in all layers of the intestine, with VIP in submucosa and mucosal plexus, and very little with nNOS.

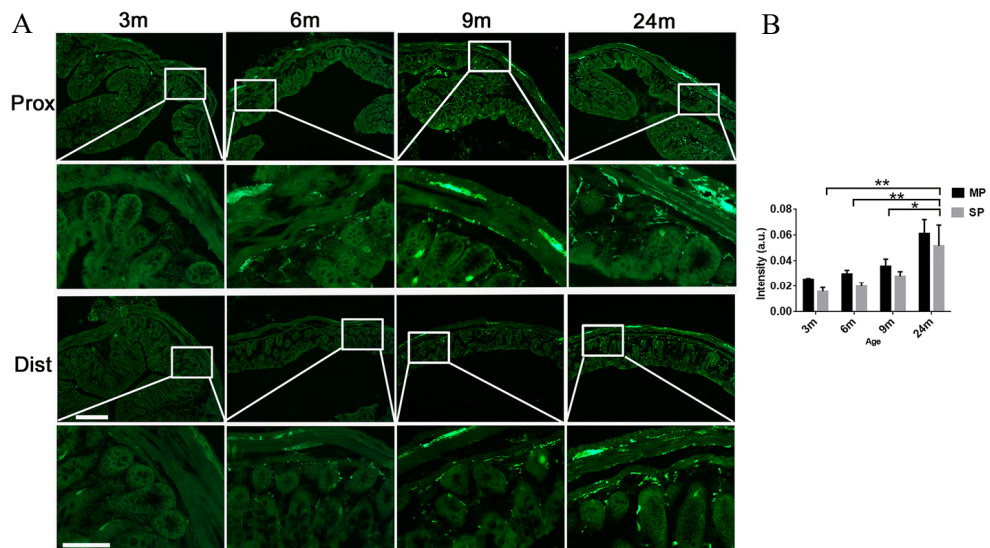


Figure 8. Age-dependent α -syn expression in the colon of the transgenic mice. (A) Representative images of α -syn-GFP transgene expression in the proximal and distal colon at 3, 6, 9 and 24 months of age. (B) Semi-quantitative analysis of GFP fluorescence intensity in the myenteric and submucosal plexus at different ages. A two-way ANOVA with Bonferroni adhoc test was used to evaluate statistical significance (** $p < 0.01$, * $p < 0.05$). Error bars in SEM. Scale bar = 250 μ m and 100 μ m in scaled up images.

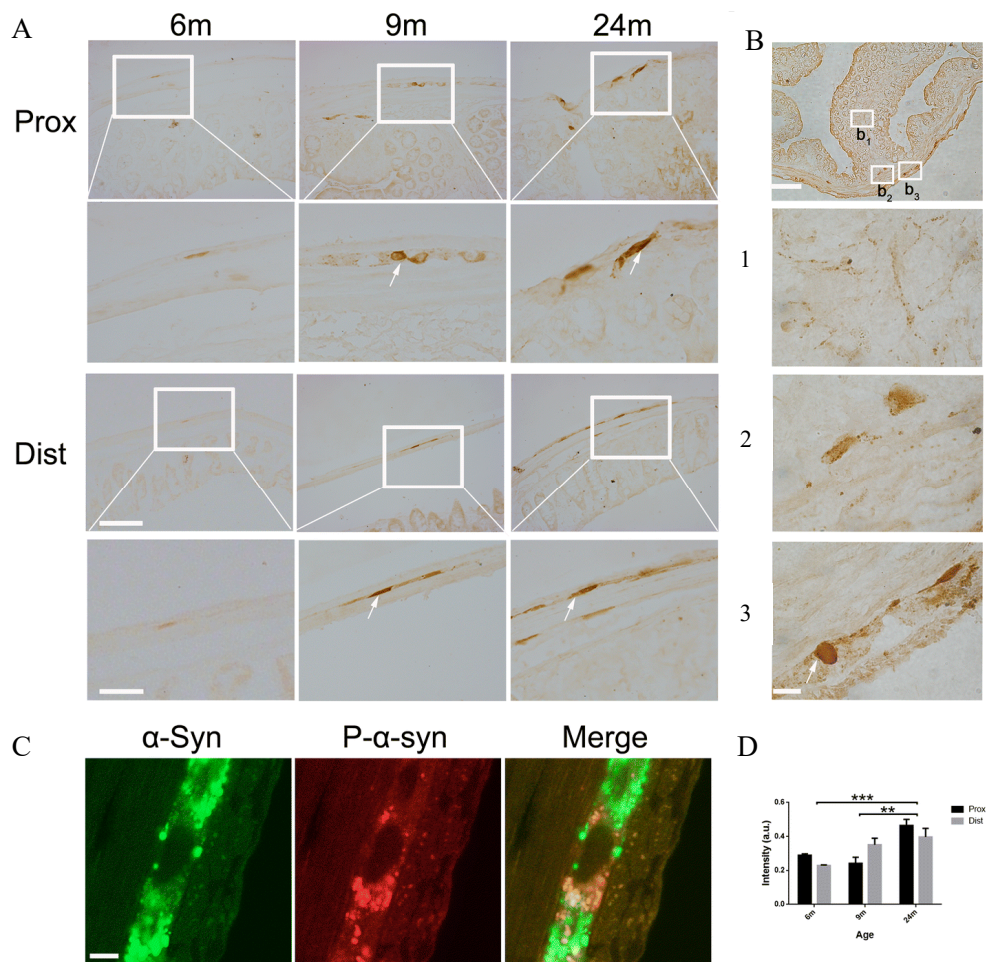


Figure 9. Age-dependent phosphorylation of α -syn in the colon of the transgenic mice as a function of age. (A) Representative images of p-syn in the proximal and distal colon at 6, 9 and 24 months of age. (B) Zoomed in images of (1) mucosal layer, (2) Meissner's plexus, and (3) Auerbach's plexus. (C) Colocalization of α -syn-GFP and p-syn. (D) Semi-quantitative analysis of p-syn intensity in Auerbach's plexus at different ages. A two-way ANOVA with Bonferroni adhoc test was used to evaluate statistical significance (*** $p < 0.001$, ** $p < 0.01$). Error bars in SEM. Scale bar = 250 μ m and 100 μ m in scaled up images in (A), 500 μ m and 50 μ m in (B) and 10 μ m in (C).

Paper III

α -Syn fibrils have been shown to act as seeds and accelerate the aggregation of prion protein (120), A β 40, A β 42 (121), and tau (122). This cross-seeding of human amyloid proteins raises the question of whether all amyloid proteins possess the ability to modulate others' aggregation. Proteins capable of assuming an amyloid conformation are found in vertebrates, fungi and bacteria (123). They often contribute to biofilm formation and virulence. The Curli proteins in *E. coli* and *Salmonella enterica*, Chaplins in *Streptomyces coelicolor*, TasA in *Bacillus subtilis*, WapA in *Streptococcus mutans*, and Phenol Soluble Modulins in *S. aureus* are all such examples. To evaluate whether any bacterial amyloid proteins could affect α -syn aggregation, we first performed a pilot experiment where we co-incubated different concentrations (0.7, 7, and 24 μ M) of several bacterial amyloid peptides (BAPs) with 70 μ M α -syn in 10 mM MES buffer pH 5.5 with 20 μ M Thioflavin T (ThT) at 37°C under quiescent conditions. We obtained these different BAPs as generous gifts from other researchers and did not subject the samples to dialysis, so differences in the buffer composition could affect the results. While α -syn alone did not start aggregating up to 150 h, α -syn incubated in the presence of two peptides started aggregating and plateaued within 40 h (Figure 10). These two samples were Phenol Soluble Modulins α 2 and α 3 (PSM α).

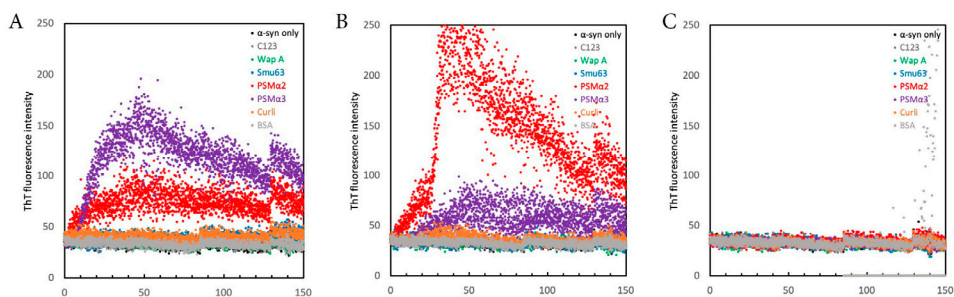


Figure 10. Pilot screen of the effects of bacterial amyloid proteins on α -syn aggregation. 70 μ M α -syn was incubated on its own or in the presence of (A) 24 μ M, (B) 7 μ M, or (C) 0.7 μ M of C123, WapA, and smu63 from *S. mutans* (124), PSM α 2 and α 3 from *S. aureus* (125), Curli from *S. enterica* (126), or bovine serum albumin. The starting α -syn was monomeric and the experiment performed in 10 mM MES with 20 μ M ThT and 0.01% NaN₃ under quiescent conditions at 37°C.

PSM α peptides were first identified in 2007 in a methicillin-resistant strain of *S. aureus* (MRSA) and were found to contribute to its virulence (127). These peptides are encoded in the core genome of *S. aureus*. In a study using an epicutaneous mouse model of *S. aureus* infection, strains of *S. aureus* deficient in PSM α induced less

skin disease and neutrophil recruitment compared to the wildtype strain (128). These peptides have also been shown to contribute to biofilm formation and are speculated to play a role in *S. aureus* enterotoxin-induced disease (129).

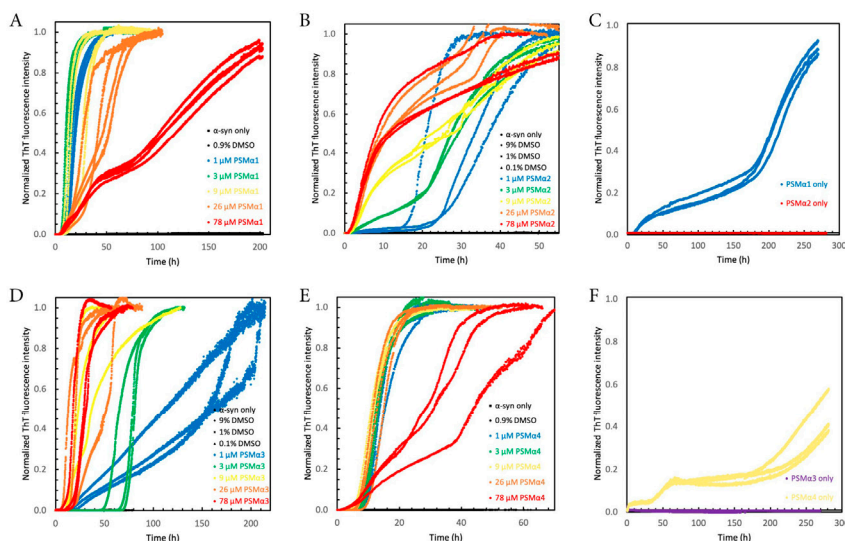


Figure 11. Aggregation of α -syn in the presence of PSM α peptides. A, B, D, E. Normalized ThT fluorescence intensity as a function of time for 25 μ M α -syn in the presence of varying PSM α 1 (A), PSM α 2 (B), PSM α 3 (D), or PSM α 4 (E) concentrations as given in the respective panel. C, F. Control experiments with only 78 μ M of PSM α 1 (blue), PSM α 2 (red), PSM α 3 (purple), or PSM α 4 (yellow). All experiments started from monomers and were performed in 10 mM Tris, 50 mM NaCl, pH 7.6 at 37 °C under quiescent conditions.

S. aureus is a prevalent skin and mucosa commensal as well as a pathogen. It has been shown to be capable of activating sensory neurons through which it modulates the immune response (76). The PSM α peptides have been shown to form pores in the neurons, causing an influx of ions, thereby activating them (130). Neutrophils, the main immune response to *S. aureus* infections, release neutrophil extracellular traps (NETs) in response to the PSM α peptides, and NETs have been shown to colocalize with human amyloids (131). As such, we deemed the PSM α peptides as interesting and wanted to investigate their impact on α -syn aggregation further.

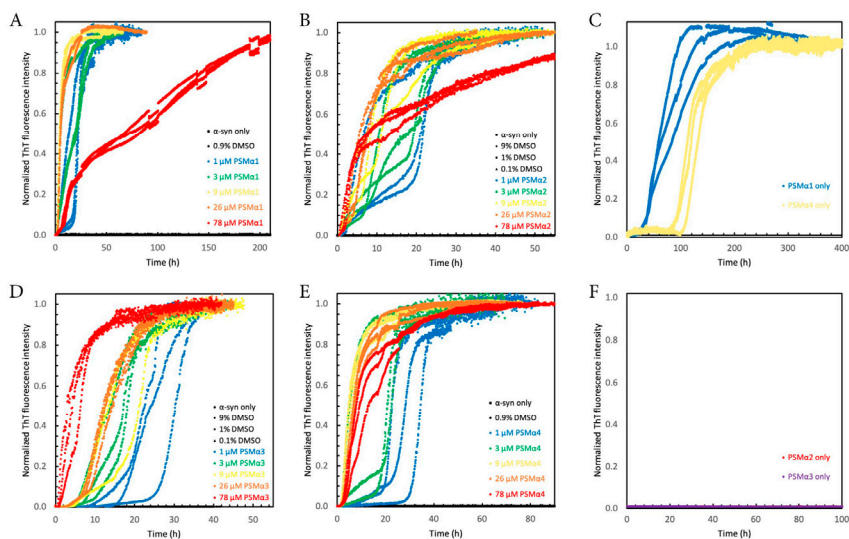


Figure 12. Aggregation of α -syn in the presence of PSM α peptides. A, B, D, E. Normalized ThT fluorescence intensity as a function of time for 25 μ M α -syn in the presence of varying PSM α 1 (A), PSM α 2 (B), PSM α 3 (D), or PSM α 4 (E). concentrations as given in the respective panel. C, F. Control experiments with only 78 μ M of PSM α 1 (blue), PSM α 2 (red), PSM α 3 (purple), or PSM α 4 (yellow). All experiments started from monomers and were performed in 10 mM MES, pH 5.5 at 37 $^{\circ}$ C under quiescent conditions.

To properly investigate the impact of a compound on α -syn's aggregation, it is important to do so under quiescent conditions in containers with PEGylated surfaces as agitation itself or the presence of nucleating surfaces such as polystyrene can catalyze α -syn aggregation, and so the effect observed under such conditions could merely be the compound's interference with the surface or a change in viscosity leading to altered air-liquid interface. We examined the effects of the four different PSM α peptides on the aggregation of 25 μ M α -syn in buffers resembling physiological conditions: i.e. 10 mM Tris, 50 mM NaCl, pH 7.6, representative of the cytoplasm and extracellular matrix, and 10 mM MES pH 5.5 resembling the lysosome. In both buffer conditions, the presence of the PSM α peptides accelerated the aggregation of α -syn, which on its own did not aggregate up to 300 h (Figure 11, 12). The dose-dependent catalysis of α -syn aggregation differed between the peptides: PSM α 2 and α 3 displayed a monotonic dose-dependence with the highest catalytic effect observed at the highest concentrations of the peptides tested, whereas PSM α 1 and PSM α 4 displayed a biphasic dose-dependence with the highest catalytic effect at 3-9 μ M. Interestingly, only PSM α 1 and PSM α 4 showed an increase in ThT fluorescence in the absence of α -syn.

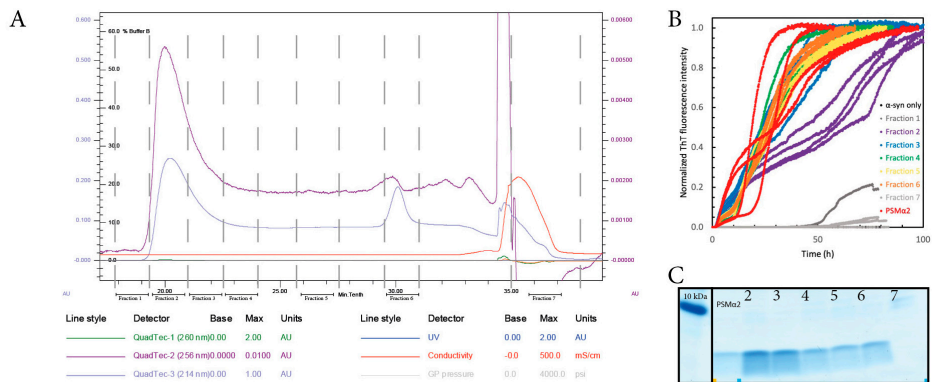


Figure 13. Aggregation of α -syn in the presence of FPLC-purified fractions of PSMA2 peptide. PSMA2 was dissolved in 6M GuHCl and purified into 10mM Tris, 50 mM NaCl, pH 7.6 using size exclusion chromatography. A. The absorbance at 214 and 256 nm was monitored and several fractions collected as indicated on the chromatogram. B. The normalized ThT fluorescence intensity as a function of time for 25 μ M α -syn aggregated in the presence of the different purified PSMA2 fractions or in the presence of 9 μ M non-purified PSMA2 in 1.1% DMSO. C. SDS-PAGE of the different fractions indicating the presence of PSMA2 in fractions 2-6 but not 7.

Since the PSM α peptides were dissolved in dimethyl sulfoxide (DMSO), we wanted to evaluate whether the observed catalysis was indeed due to the peptides. To do so, we dissolved PSM α 2 in 6 M GuHCl and 10 mM MES pH 5.5 and then repurified it into the Tris buffer using size exclusion liquid chromatography. Different samples from the purified peptide were added to 25 μ M α -syn in the presence of 20 μ M ThT and incubated at 37°C under quiescent conditions. All fractions containing PSM α 2 peptide, as verified by a SDS-PAGE of the fractions, induced α -syn aggregation (Figure 13). We could thus conclude that the observed catalysis was specific to the PSM α peptides.

To verify that α -syn had indeed aggregated, different samples were immunogold labeled with an anti- α -syn antibody and examined by transmission electron microscopy (TEM). Indeed, α -syn incubated with any of the PSM α peptides showed fibrillar aggregates labeled by the anti- α -syn antibody (Figure 14). Even α -syn incubated alone or in the presence of DMSO did show some smaller fibrillar aggregates: However, these were fewer. Additionally, these samples showed a higher background labeling, perhaps indicating a higher monomeric content, in agreement with the ThT data. When these samples were subsequently added the HEK cells overexpressing the A53T variant of α -syn fused to GFP, the co-incubated materials induced aggregate formation and phosphorylation of α -syn to a higher extent than either α -syn or PSM α peptides incubated on their own did (Figure 15).

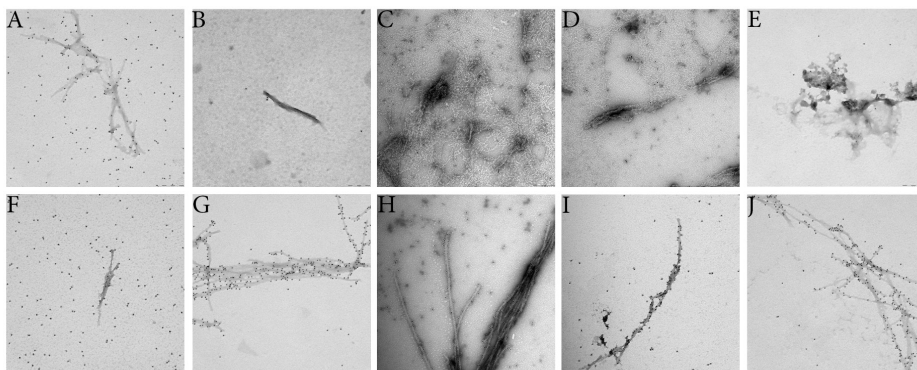


Figure 14. Electron microscopic images. TEM micrographs at 60000 times magnification of samples taken at the plateau of aggregation reactions of 25 μ M α -syn (A), 78 μ M PSMa1 (B), PSMa2 (C), PSMa3 (D), PSMa4 (E) or of 25 μ M α -syn with 1.1% DMSO in the absence (F) or presence of 9 μ M (G) PSMa1, (H) PSMa2, (I) PSMa3, or (J) PSMa4 peptides. All experiments started from monomers and were performed in 10 mM Tris, 50 mM NaCl, 0.01% NaN₃ pH 7.6 at 37 °C under quiescent conditions. After deposition on the grids, the samples were labelled by an anti- α -syn primary antibody and a secondary antibody coupled to 10 nm gold nanoparticles. Scale bar = 200 nm

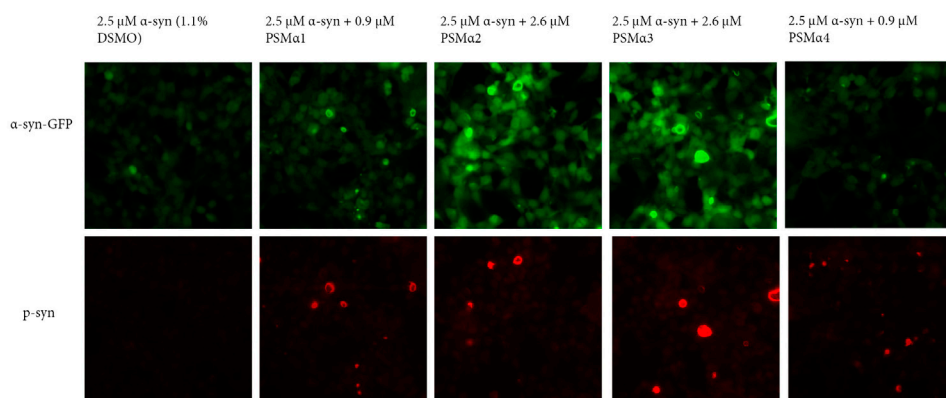


Figure 15. Seeding in HEK A53T-GFP cells. HEK cells were stained for α -syn phosphorylated at ser129 and a Cy3-conjugated secondary antibody after 48 hour-treatment with α -syn aggregated in the absence or presence of PSMa peptides at different concentrations. Representative images from one well from each treatment condition are shown

Having established that α -syn had aggregated, we wanted to model the kinetic data. When only primary nucleation and elongation were accounted for in the model, the resulting curves were too shallow to fit the ThT curves, and so secondary nucleation had to be added into the equation (Figure 16). Secondary nucleation is intrinsic to α -syn and the peptides do not appear to inhibit this process. We expect the peptides induced aggregation by heterogeneous primary nucleation, after which the formed α -syn seeds auto-catalyzed the aggregation of the remaining monomers.

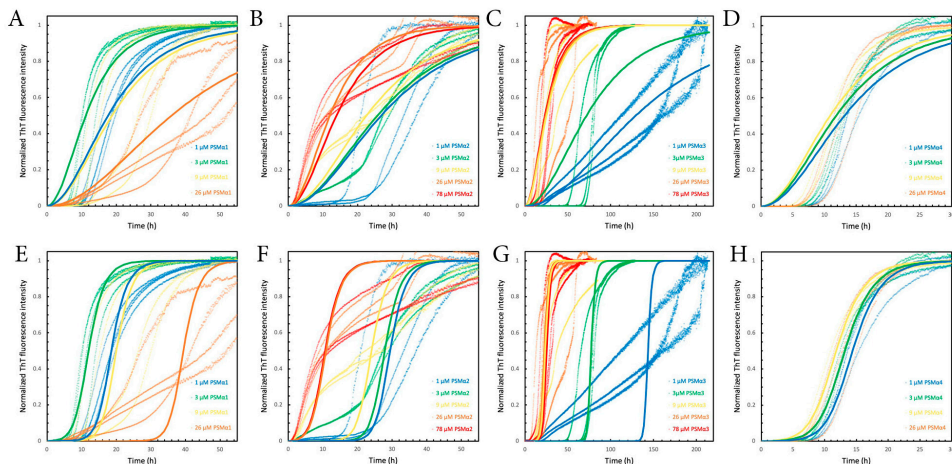


Figure 16. Fitting of models of nucleation and elongation to aggregation kinetics of α -syn in the presence of PSM α peptides. The ThT fluorescence intensities as a function of time of 25 μ M α -syn aggregation induced by varying PSM α 1 (A, E), PSM α 2 (B, F), PSM α 3 (C, G), or PSM α 4 (D, H) concentrations (μ M) were fitted to models of primary nucleation and elongation (A, B, C, D) or to models of primary nucleation, elongation and secondary nucleation (E, F, G, H). The dotted lines are the normalized ThT fluorescence intensities and the solid lines are the fits as calculated by Amylofit. All experiments started from monomers and were performed in 10 mM Tris, 50 mM NaCl, 0.01% NaN₃, pH 7.6 with 20 μ M ThT at 37 °C under quiescent conditions.

Next, we performed peptide arrays wherein 10-residue peptides corresponding to the PSM α sequences were immobilized onto arrays and then probed with Alexa 488-labelled α -syn. PSM α 1 and α 4 showed no particularly strong interaction with α -syn, but PSM α 2 and α 3 did (Figure 17), perhaps explaining the differences in concentration-dependent catalysis previously observed.

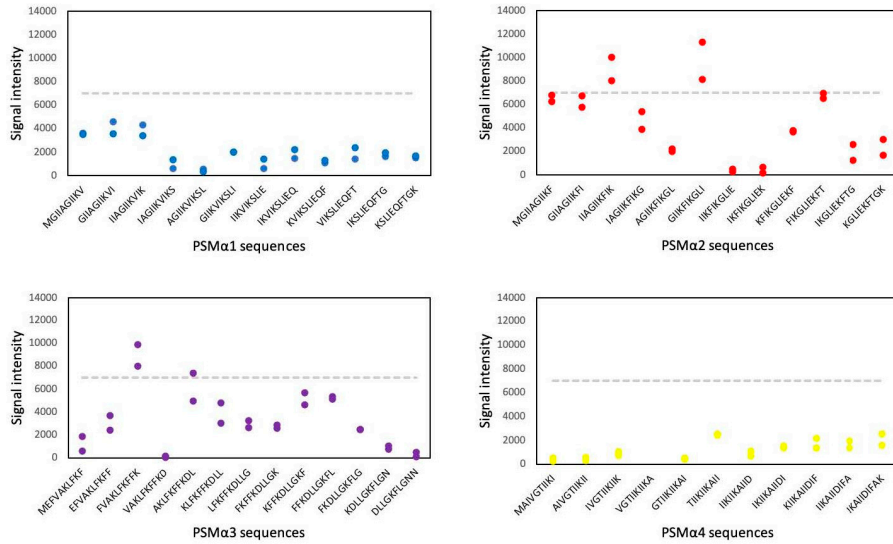


Figure 17. Arrays of PSMa sequences. Alexa-fluor488-labeled- α -syn was added onto arrays coated with different 10-meric peptide sequences of each of the 4 studied PSMa peptides as per the figures. The signal intensity was measured and plotted for each sequence, with the dashed line at 7000 indicating the threshold value above which, α -syn was deemed to bind to a peptide. Each experiment was performed twice.

We next evaluated whether a *S. aureus* infection could trigger α -syn aggregation *in vivo*. To do so, we obtained skin, spinal cord and brain samples from Isaac Chiu's lab, working with MRSA infection in mice. Three C57bl/6 mice had been epicutaneously infected with MRSA for five days before they were sacrificed and the samples post-fixed in 4% phosphate-buffered paraformaldehyde. Control mice had been similarly treated with phosphate buffered saline (PBS). The skin samples were paraffin-embedded and sectioned at 6 μ m thickness. The MSA infected samples showed increased reactivity to an antibody against endogenous mouse α -syn, localizing to the area of the lesion (Figure 18). The spinal cords and brains samples were sectioned at 30 μ m thickness using a freezing microtome. The samples did not show increased α -syn and only a moderately increased Iba-1 reactivity, perhaps due to the experiment's short duration. We are now in the process of establishing a similar MRSA-infection model on our BAC-SNCA-GFP mice.

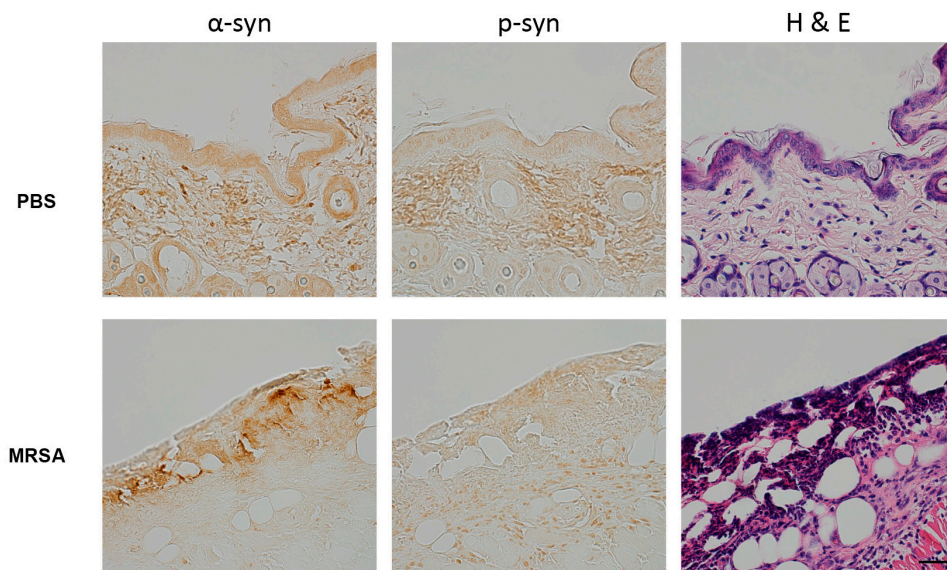


Figure 18. MRSA infection stimulates endogenous α -syn expression. C57bl/6 mice were infected with MRSA or PBS for 5 days after which they were sacrificed and the lesioned skin collected. Endogenous mouse α -syn expression increased at the site of the lesion but was not phosphorylated. Scale bar = 20 μ m.

Paper IV

DMSO is polar and aprotic, which makes it a widely used solvent for hydrophobic substances. It is regularly used as a cryoprotectant for cells, in studies examining the effect of compounds on α -syn aggregation, and as a solvent for cross-linkers, which have been used to stabilize α -syn's physiological state. There is already some evidence suggesting that the presence of 1% (v/v) of DMSO during the aggregation of α -syn results in the formation of an intermediary species (132). As such, we wanted to investigate the effect of DMSO on α -syn aggregation in different model systems. 35 μ M α -syn in PBS with 40 μ M ThT was incubated alone or in the presence of 1%, 5% or 10% DMSO (v/v) at 37°C and 1050 rpm. A dose-dependent shortening of the lag phase was observed with α -syn aggregated in the presence of 10% DMSO already reaching a ThT plateau after four days. In contrast, α -syn incubated on its own did not show an increase in ThT fluorescence until ten days after the start of the experiment (Figure 19). When this experiment was repeated with 25 μ M α -syn in the absence or presence of DMSO at 37°C and quiescent conditions in non-binding plates, no increase in ThT could be observed for up to 350h in PBS or Tris buffer. To examine whether DMSO would affect α -syn in the presence of nucleating surfaces, 25 μ M α -syn in Tris was incubated on its own or in the presence of different concentrations of DMSO at 37°C under quiescent conditions in polystyrene plates. Under these conditions, DMSO accelerated α -syn aggregation, with the ThT fluorescence plateauing after 140 h in the presence of 9%, and after 200h in the presence of 3%. The lower concentrations did not consistently accelerate the aggregation compared to α -syn in the absence of DMSO (Figure 20). These data indicate DMSO could accelerate α -syn aggregation in the presence of other nucleating factors but was not potent enough to accelerate the aggregation of this concentration of α -syn under quiescent conditions within the timeframe of the experiment.

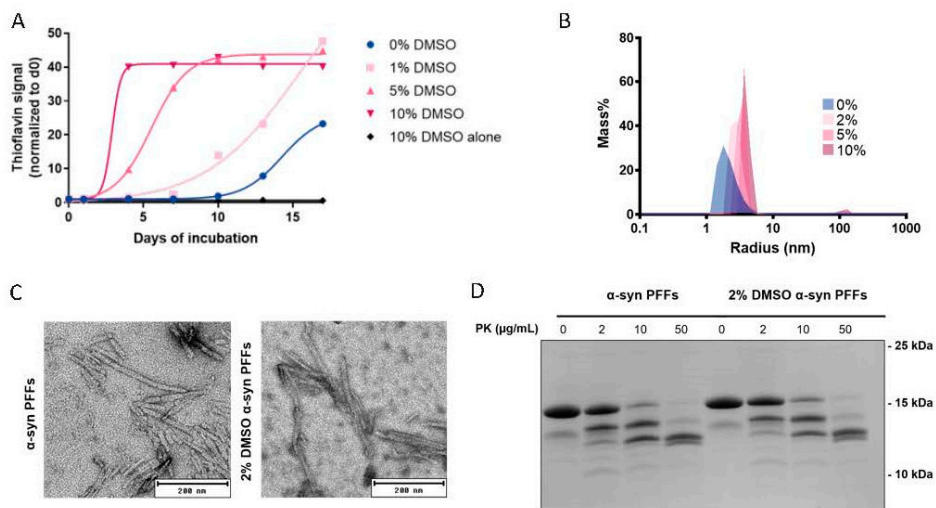


Figure 19. DMSO accelerates α -syn aggregation under agitation conditions. (A) 35 μ M α -syn in PBS and 40 μ M ThT was incubated in the absence or presence of different concentrations of DMSO at 37°C and 1050 rpm. (B) Dynamic light scattering analysis of 35 μ M α -syn incubated for 1h with or without DMSO reveals a concentration-dependent shift in mass distribution towards a larger hydrodynamic radius in the presence of DMSO. (C) TEM images of α -syn aggregated in the absence or presence of 2% DMSO. Scale bar = 200 nm. (D) Subsequent proteinase K digestion of these fibrils reveals similar proteolytic cleavage patterns for α -syn aggregated in the absence or presence of 2% DMSO.

α -Syn aggregated in the presence or absence of DMSO was then examined by TEM and Western blotting following proteinase K digestions. Both the structure of the fibrils and the proteolytic cleavage patterns indicated α -syn aggregated in the presence of DMSO was similar to that aggregated in its absence. To elucidate the mechanism underlying DMSO's effect on α -syn aggregation, 35 μ M α -syn in PBS was incubated for 1h in the absence or presence of DMSO and the samples examined by dynamic light scattering (DLS). A dose-dependent increase in particle size could be observed (Figure 19). DMSO can mimic membranes for transmembrane proteins, having dipole-dipole interactions with polar, positively charged amino acid side chains and forming hydrophobic pockets towards hydrophobic side chains (133). This could result in folding of α -syn, accounting for its increased radius.

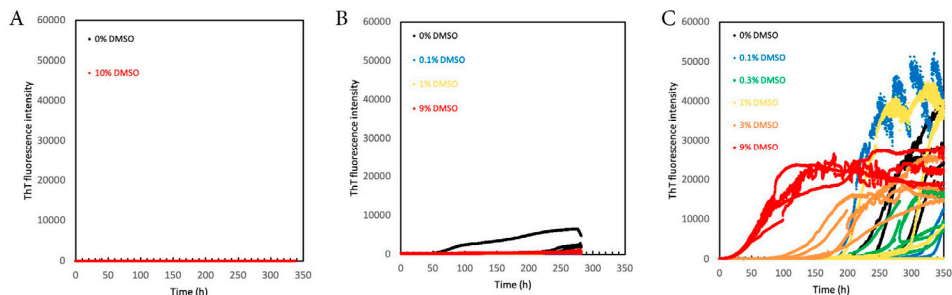


Figure 20. DMSO accelerates α -syn aggregation in the presence of nucleating factors. (A) 25 μ M α -syn in PBS, 0.01% NaN₃ and 20 μ M ThT and was incubated in the absence or presence of 10% DMSO in non-binding plates. No increase in ThT fluorescence was observed over the timeframe of the experiment. (B). 25 μ M α -syn in 10 mM Tris, 50 mM NaCl, 0.01% NaN₃, and 20 μ M ThT and was incubated in the absence or presence of different concentrations of DMSO in non-binding plates. No increase in ThT fluorescence was observed over the timeframe of the experiment. (C) 25 μ M α -syn in 10 mM Tris, 50 mM NaCl, 0.01% NaN₃ and 20 μ M ThT and was incubated in the absence or presence of different concentrations of DMSO in polystyrene plates. 9% and 3% DMSO shortened the lag phase for α -syn but no acceleration of aggregation could be observed for the lower concentrations of DMSO compared to α -syn incubated on its own.

Next, to examine the effect of DMSO on α -syn in cultured cells, neuronal SH-SY5Y cells expressing α -syn under control of the Tet-off system were differentiated using retinoic acid, and α -syn overexpression induced 24 h post-seeding, at which point different concentrations of DMSO were added. The cells were treated with DMSO for seven days and α -syn aggregate formation was evaluated. Even though the lowest concentration of DMSO (0.1% v/v) showed a trend towards increased immunoreactivity when probed with a conformation-specific anti- α -syn antibody (MJF-14-6-4-2), only effects induced by concentrations of 0.25% and above reached statistical significance (Figure 21). No significant increase in p-syn could be observed in any treatment conditions.

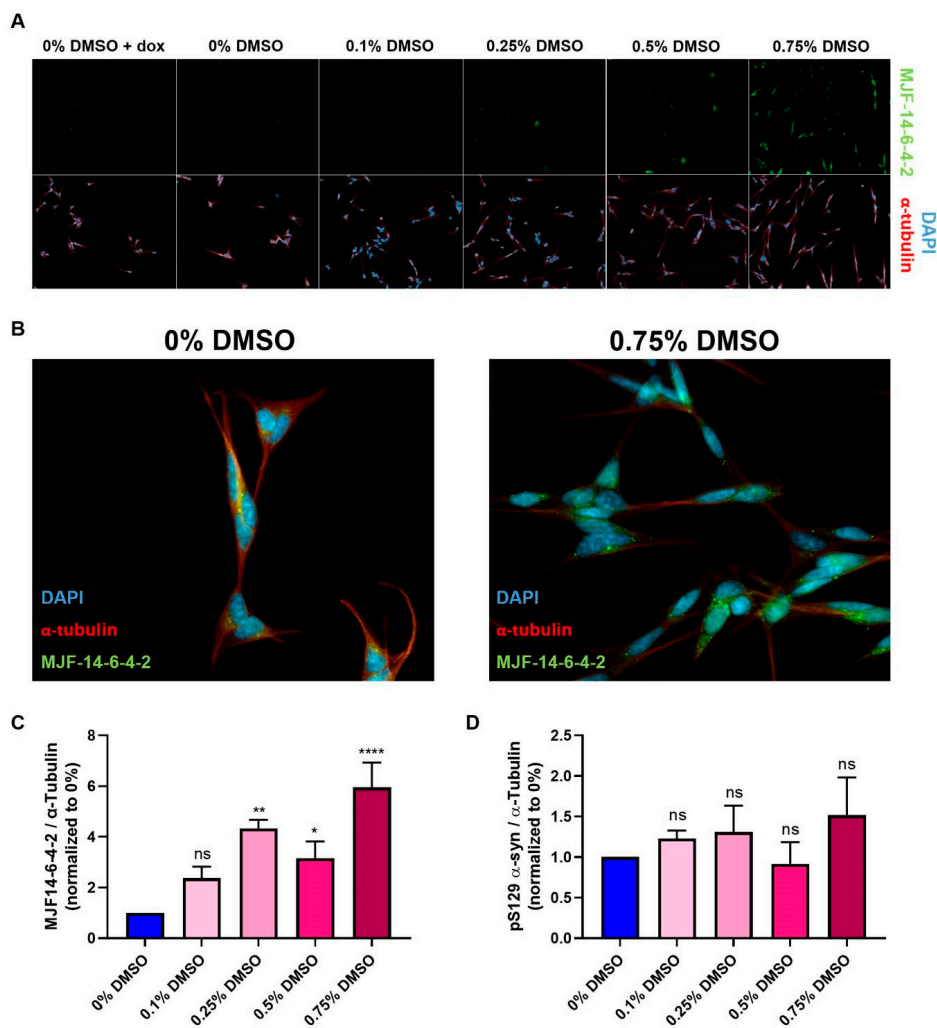


Figure 21. DMSO treatment induces α -syn multimerization in cells (A) SH-SY5Y ASYN cells were treated with dox to suppress α -syn expression (- α -syn) or relieved from dox treatment to induce α -syn overexpression. Cells relieved from dox were treated with increasing amounts of DMSO (0%, 0.1%, 0.25%, 0.5% or 0.75%) for 7 days prior to fixation, and visualized using DAPI (blue), MJFR-14-6-4-2 (green) or α -tubulin (red). To stop mitosis, the SH-SY5Y ASYN cells were treated with retinoic acid (10 μ M final concentration) during the experiment. (B) High magnification image of α -syn expressing SH-SY5Y ASYN cells treated with 0%-(left) or 0.75% (right) of DMSO for 7 days prior to fixation, and visualization using DAPI (blue), MJFR-14-6-4-2 (green) and α -tubulin (red). (C) Quantification of area of MJFR-14-6-4-2 signal from individual coverslips relative to area of α -Tubulin signal in α -syn expressing cells treated with increasing amounts of DMSO (0%, 0.1%, 0.25%, 0.5% or 0.75%) for 7 days ($n = 4$, with ~ 10 images for each condition in each experiment, * $p < 0.05$, ** $p < 0.01$, **** $p < 0.0001$, one-way ANOVA followed by Dunnett's multiple comparison test). (D) Quantification of area of anti-phospho-S129 α -syn signal from individual coverslips relative to area of α -Tubulin in α -syn expressing cells treated with increasing amounts of DMSO (0%, 0.1%, 0.25%, 0.5% or 0.75%) for 7 days ($n = 3$ with ~ 8 images for each condition in each experiment, one-way ANOVA followed by Dunnett's multiple comparison test).

To examine whether similar effects could be observed *in vivo*, F28 mice overexpressing human wildtype α -syn under the mouse's endogenous SNCA promotor (similar to our BAC-SNCA-GFP mice but without the GFP) and C57bl/6 mice were treated with 10% or 30% DMSO or vehicle (PBS) by oral gavage for 14 consecutive days after which they were sacrificed. Neither duodenum and ileum, nor striatum and substantia nigra showed increased immunoreactivity to MJF-14-6-4-2. Additionally, no decrease in tyrosine hydroxylase (TH) immunoreactivity could be observed in the brain (Figure 22). This could be due to the animal's young age (three months at the start of the experiment), such that α -syn had not yet accumulated in large enough concentrations to be affected by environmental toxins. Alternatively, even though DMSO is known to be absorbed *in vivo* (134), the presence of chaperones could inhibit its effect on α -syn.

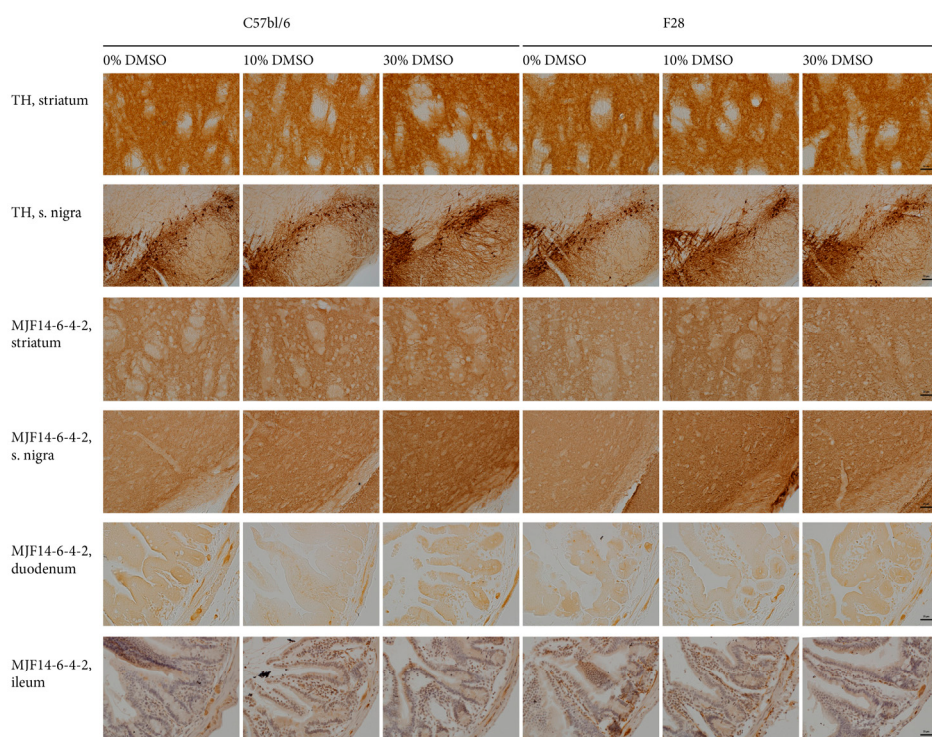


Figure 22. Oral treatment with DMSO does not induce α -syn aggregation *in vivo*. Free floating 30 μ m sections of brain tissues from striatum or substantia nigra or paraffin embedded sections of duodenum and ileum from C57BL/6 and F28 mice. Twelve wildtype C57bl/6 and twelve transgenic F28 mice were divided into three groups with four in each and treated with water (0% DMSO), 10% DMSO (1 g/kg bodyweight) or 30% DMSO (3 g/kg bodyweight) for 14 days prior to sacrificing and tissue collection. Striatum or substantia nigra sections from all animals were stained with an anti-tyrosine hydroxylase antibody and with the MJFR-14-6-4-2 antibody ($n = 4$ for each condition). The duodenum and ileum samples from all animals were stained with the MJFR14-6-4-2 antibody. $N = 4-6$ sections per segment (s2, s5, s8) were analyzed for the intestinal samples and one series of brain sections spanning the entirety of the brain from OB to beginning of cerebellum (30 μ m sections, 10 series = 300 μ m distance between the sections for each series) for each animal. Scalebar = 20 μ m for striatum, duodenum and ileum and 50 μ m for substantia nigra.

Discussion and Future Perspectives

In the work presented in this thesis, we have aimed to understand the complexities underlying α -syn aggregation and pathology. We have studied aggregated α -syn in different brain regions from patients with different synucleinopathies, in the colon of transgenic mice, and *in vitro* in the presence of bacterial amyloid peptides and DMSO.

Synucleinopathies are common neuropathologies that appear in different disease presentations, with an underlying pathological accumulation of α -syn aggregates. Because α -syn fibrils isolated from patients with different synucleinopathies have shown to induce varying toxicities and are now touted as different strains, we sought to investigate whether the α -syn within these aggregates were differently processed. We were also curious whether brain regions affected at different stages of the diseases would have altered α -syn signatures due to cellular dysfunction. Many sections, with α -syn pathology, as evidenced by other antibodies, did not show much immunoreactivity when probed with the antibody targeting residues 34-45. This epitope would be affected in alternative splicing products. Many of the residues in this epitope are also part of the β -sheet and could potentially be hidden in certain conformations. Mass spectrometric analyses of samples that displayed different immunoreactivity to this antibody would be very interesting. The observed C-terminal truncation abundance in PD was not brain-region specific, indicating this could be an early modification to the protein. That larger aggregates in MSA patients were not composed exclusively of C-terminally truncated α -syn perhaps indicates a highly efficient seed capable of templating different forms of α -syn. Elucidating the spatio-temporal modifications of α -syn will be valuable in understanding disease progression. Additionally, this information could aid in designing immunotherapy antibodies to be used in clinical settings. If an epitope is hidden or truncated, an antibody designed towards it might not be an effective therapy.

While synucleinopathies have historically been seen as primarily brain disorders, non-motor symptom onset preceding diagnosis by many years has prompted the study of peripheral organs. Because many models of synucleinopathy have primarily focused on the CNS, even limiting inflammation to the CNS, findings made in those models have not translated into clinical settings. Models accounting for peripheral involvement would also be needed to better capture the entirety of the underlying pathology. To evaluate whether experimental models of synucleinopathy

could capture this peripheral involvement, we studied the colon of a transgenic mouse expressing human α -syn under the control of the mouse's endogenous SNCA promotor. We would expect this model to show accumulation of human α -syn only in those tissues where it would normally be expressed. In agreement with PD symptomatology, these mice showed signs of constipation early in the disease progression. They also showed age-dependent accumulation and phosphorylation of α -syn. This did coincide with α -syn accumulation in the brain as previously characterized, indicating peripheral and CNS involvement happens in tandem, at least in a monogenetic model of the disease. Since the publication of that study, biopsy samples from PD patients have confirmed the presence of α -syn in the enteric nervous system and evaluation of whether this could be a biomarker to detect PD prior to symptom onset is ongoing. Biomarkers for early detection would be key in studying preventative and early therapeutic measures.

Because of this peripheral involvement and the idiopathic nature of most synucleinopathies, environmental triggers of pathology have been proposed. Here, inspiration from the study of A β , which is triggered by pathogens, has been taken. Indeed a few studies have reported that infections can trigger α -syn aggregation (74, 75). We were interested in exploring the mechanisms by which α -syn aggregation could be triggered by microorganisms and particularly by bacterial amyloid proteins for several reasons: firstly, many bacteria express these functional amyloids and they contribute to biofilm formation and virulence, thus indicating they would be in contact with the host organism; secondly, dysbiosis has been shown in PD patients with the intestinal microbiome possibly playing a causative role in driving α -syn pathology; and thirdly because α -syn has already been shown to cross-seed with other amyloid proteins. The studied PSM α peptides significantly accelerated α -syn aggregation in the absence of any other nucleating factors. The differences in concentration dependence between the peptides further indicate that the effects are sequence-specific. α -Syn aggregation in the presence of the peptides could be an underlying mechanism for its anti-microbial activity against *S. aureus*. In a pilot study, we have observed accumulation of endogenous mouse α -syn in the skin at the lesion site as an effect of *S. aureus* infection. It has already been established that the peptides participate in virulence, but their expression patterns in commensal situations are unknown. One study has shown biofilm formation, which PSM α peptides have been shown to contribute to, is induced upon treatment with low dose antibiotics (135). An infection-based model of synucleinopathy is interesting but studying infections underlying initiation of disease might prove difficult as synucleinopathies often take many years to progress until diagnosis, at which point evidence of the infection will likely have resolved. As α -syn aggregates have been shown capable of propagating from the periphery, the causative microorganism need not directly interact with the CNS. Different microorganisms underlying synucleinopathies could also explain the varying symptomatology: causative agent

and site of infection could contribute to different spreading patterns. As Alzheimer's disease is now also speculated to be initiated by pathogens, it is interesting to ask whether certain organisms always induce preferential aggregation of either α -syn or A β or whether the patient's underlying predisposition is what ultimately determines which protein aggregates.

Our peptides were dissolved in DMSO, as are many other compounds used to study α -syn in its physiological form and during aggregation. As such, we were curious whether DMSO itself affected α -syn. We incubated α -syn with varying concentrations of DMSO, and found that in the presence of other nucleating factors, DMSO could accelerate α -syn aggregation. When examined by DLS, we could see that DMSO increased the radius of α -syn particles. This might be an effect of DMSO's dual solvent properties, contributing to a screening of electrostatic repulsions between different α -syn molecules. This in itself could have implications for the observed size of α -syn when isolated from tissues and cells in the presence of DMSO. When cells were treated with DMSO, they too formed p-syn aggregates. This is particularly concerning as DMSO is used as a cryoprotectant in cell culture.

Our current work highlights the complexities of α -syn aggregation and the need for scrutiny when studying it. Future studies need to use models reflective of this complexity when dissecting the contributions of various systems to the pathology and elucidating the physiological role of α -syn. The lack of effective therapeutic strategies developed since the descriptions of these diseases several decades ago indicates the extensive research and resources invested into this field might have been misdirected. Studies on single mechanisms need to be properly contextualized and conclusions not hastily drawn.

Materials and Methods

Human tissues and animal experiments

Human post-mortem brain tissue

Formalin-fixed paraffin-embedded patient samples were obtained either from the Division of Oncology and Pathology of Lund University Hospital or from the brain bank at Mount Sinai as indicated by Table 1. Samples were sectioned at 5 μ m thickness using a paraffin microtome (Galileo AUTO) and mounted onto ThermoFrost glass slides for further processing.

Animals

All animal experiments were conducted in accordance with ethical permits approved by the Animal Welfare and Ethics committee of Lund/Malmö (ethical permit numbers M73/16 and the amendment 5.8.18-03524/2020).

C57bl/6, BAC-SNCA-GFP and F28 mice were used in the studies in this thesis.

Animals were housed in cages with access to food and water ad libitum under a 12h light/ 12 hour dark cycle.

Intestinal transit time

Carmin dye was administered to C57bl/6 and BAC-SNCA-GFP mice of different ages by oral gavage. The mice were observed until the dye was detected in the stool and the transit time recorded.

The mice were then sacrificed by an intraperitoneal injection of pentobarbital and transcardially perfused by 0.9% saline. Brains and GI tracts were dissected and either snap frozen in liquid nitrogen and then stored at -80°C until processed or post-fixed in 4% phosphate buffered paraformaldehyde pH 7.4 for 24-48 hours and then either cryopreserved in 30% sucrose or dehydrated in a series of ethanol changes prior to paraffin embedding.

SYNUCLEINOPATHY	NUMBER OF CASES	PATIENT INFORMATION	BRAIN REGIONS	SOURCE
PD	1		Occipital cortex	Department of Pathology, Lund University Hospital
			Hippocampus	
PD (MSA-LIKE WHITE MATTER DISEASE)	1		Frontal cortex	
			Parietal Cortex	
			Hippocampus	
PDD (HEREDITARY)	1		Mesencephalon	Mount Sinai Brain Bank
DLB (CORTICAL)	1		Frontal cortex	
			Amygdala	
			Hippocampus	
			Anterior Cingulate Cortex	
MSA	1		Hippocampus	
			Pons	
PD	4	84-year old white female	Hippocampus	
		86-year old white female	Substantia Nigra	
		82-year old white female	Amygdala	
		84-year old white male	Putamen	
DLBD	4	87-year old white female	Cortex (Brodmann, BM 9/46)	
		77-year old white male	Cerebellum	
		77-year old white female		
		86-year old black female		
MSA	2	69-year old asian female		
		69-year old white male		
CONTROL	4	67-year old black female		
		66-year old white male		
		69-year old white male		
		81-year old hispanic female		

Table 2. List of samples analyzed in the first study

DMSO administration

4 month old F28 and C57bl/6 mice were treated with PBS or DMSO dissolved in PBS to a final concentration of 10% or 30% (v/v). The solutions were administered by oral gavage (10 ml/kg) once daily for 14 days. 1 day after completed treatment, the mice were sacrificed and their tissues processed as described above.

Tissue sectioning

Brains were sectioned coronally at 30 μm thickness using a freezing microtome and stored in Walter's antifreeze solution. The free-floating sections were then washed in PBS and further processed without any antigen retrieval.

Cryopreserved intestinal segments were transversally cut at 10 μm thickness using a cryostat and mounted onto gelatin-coated glass slides.

Paraffin-embedded intestinal segments were transversally cut at 6 μm thickness using a paraffin-microtome and mounted onto Superfrost glass slides.

Immunohistochemistry

Paraffin-embedded sections (human brain samples and mouse intestines) were dried at 60°C for 1 hour followed by deparaffinization in xylene and a series of ethanol baths. Prior to heat-mediated antigen retrieval, these sections were treated with 80% formic acid for 10 mins and subsequently washed in dH₂O.

Heat mediated antigen retrieval was performed on paraffin-embedded tissues and frozen, mounted intestinal sections in 0.01M Citrate buffer (pH 6.0 for human samples, 8.5 for mouse samples) for 40 minutes at 95°C. Samples were allowed to cool and washed in PBS.

Endogenous peroxidase was quenched by treating all samples (including free-floating brain sections) with a 3% H₂O₂ in PBS solution for 15 minutes at room temperature. Samples were washed in PBS and preincubated in a solution containing normal serum, BSA and Triton X100. Primary and secondary antibodies were diluted in the blocking buffer at the dilutions indicated by Table 3 and sequentially added to the samples. Signal was amplified by ABC (VEPK-6100) solution and developed with DAB (SK-4100). Free-floating sections were mounted onto gelatin coated slides. Sections were dehydrated in ethanol and cleared in xylene then coverslipped with pertex.

Immunofluorescence

For immunofluorescent and double-labelling, samples were similarly treated but without quenching of endogenous peroxidase or amplification of signal by ABC and developing by DAB. After washing post secondary antibody incubation, autofluorescence was quenched with 1% Sudan Black. After washing, samples were coverslipped with PVA/DABCO.

ANTIBODY	EPITOPE	SOURCE	HOST ANIMAL	DILUTION USED
EGT 403	α -syn residues 1-5	EPFL	Mouse	1:200
EGT 410	α -syn residues 1-10	EPFL	Mouse	1:500
BL-LASH-N-TERM	α -syn residues 1-20	EPFL	Rabbit	1:200-2000
BL-LASH-34-45	α -syn residues 34-45	EPFL also available at Biolegend (849101)	Mouse	1:500-2000
BL-LASH-80-96	α -syn residues 80-96	EPFL also available at Biolegend (848301)	Mouse	1:2000
SYN-1	α -syn residues 91-99	BD Biosciences (BD610787)	Mouse	1:500
4B12	α -syn residues 103-108	Biolegend (807804)	Mouse	1:500
EGT 406	α -syn residues 108-120	EPFL	Mouse	1:500
EGT 408	α -syn residues 107-140	EPFL	Mouse	1:500
FAR C-TERMINAL	α -syn residues 134-138	Abcam (ab131508)	Rabbit	1:2000
PS129	α -syn phosphorylated at Serine 129	Abcam (ab51253)	Rabbit	1:200-1000
MJF14	Conformation-specific anti- α -syn	Abcam (209538)	Rabbit	1:5000-25,000
D37A6	Endogenous mouse α -syn	Cell Signal (4179)	Rabbit	1:1000
SYN211	α -syn residues 121-125	Santa Cruz Biotechnology (12767)	Mouse	1:200-1000
CALRETININ	N-terminus of human calretinin	Santa Cruz Biotechnology (11644)	Goat	1:400
NNOS	Neuronal NOS	Abcam (76067)	Rabbit	1:400
VIP	Vasoactive intestinal peptide	Abcam (22736)	Rabbit	1:800
α-TUBULIN	α -Tubulin	Sigma Aldrich (T9026)	Mouse	1:1000
TH	Tyrosine Hydroxylase	GeneTex (113016)	Rabbit	1:30,000
BIOTINYLATED ANTI-MOUSE	Mouse IgG (H+L)	Vector Laboratories (BA2001)	Horse	1:500
BIOTINYLATED ANTI-RABBIT	Rabbit IgG (H+L)	Vector Laboratories (BA1000)	Goat	1:500
CY3-ANTI-MOUSE	Mouse IgG (H+L)	Jackson Immuno Research (715-165-150)	Donkey	1:400-1000
CY3-ANTI-RABBIT	Rabbit IgG (H+L)	Jackson Immuno Research (711-175-152)	Donkey	1:400-1000
CY5-ANTI-RABBIT	Rabbit IgG (H+L)	Jackson Immuno Research (711-175-152)	Donkey	1:400-1000
ALEXA488-ANTI-GOAT	Goat IgG (H+L)	Jackson Immuno Research (705-545-147)	Donkey	1:400-1000
GOLD-ANTI-MOUSE	Mouse IgG (H+L)	Ted Pella (15751)	Goat	1:50
HRP-ANTI-MOUSE	Mouse IgG (H+L)	Dako (P0260)	Rabbit	1:1000
HRP-ANTI-RABBIT	Rabbit IgG (H+L)	Dako (P0217)	Swine	1:1000

Table 3. List of antibodies used in this thesis

Image acquisition

Brightfield images were acquired using an Olympus BX microscope. Fluorescent images were acquired using a Leica SP8 confocal microscope.

Biochemical and molecular methods

Alpha-synuclein production and purification

Recombinant full-length wildtype human α -syn was produced as previously described (136). In brief, *E. coli* were transformed with an inducible human α -syn cDNA containing pET3a plasmid. α -Syn production was induced by treatment with IPTG. The bacteria were pelleted and α -syn purified by heat treatment, ion exchange and gel filtration chromatography. These samples were lyophilized and stored at -80°C until use.

PSM α peptide production

The four different PSM α peptides were produced by chemical synthesis and isolated by reversed-phase high-performance liquid-chromatography to 95% purity by EMC microcollections GmbH with the following sequences:

PSM α 1: Formyl-MGIIAGIIKVIKSLIEQFTGK

PSM α 2: Formyl-MGIIAGIIKFIKGLIEKFTGK

PSM α 3: Formyl-MEFVAKLKFKKDLLGKFLGNN

PSM α 4: Formyl-MAIVGTIIKIIKAIIDIFAK

They were purchased as lyophilized peptides and stored at -80°C until use.

Kinetics experiments

Prior to each kinetics experiment, lyophilized α -syn was solubilized in 6M GuHCl in 10 mM MES buffer and a pure monomer solution isolated by size exclusion chromatography on a Superdex 75 column into desired buffer (10mM Tris 50 mM NaCl, 10 mM MES, or 0.1 M PBS). Purified monomer solution was stored on ice to prevent aggregation. Absorbance was measured at 280 nm and concentration calculated using an extinction coefficient of $5960 \text{ M}^{-1}\text{cm}^{-1}$.

PSM α peptides were dissolved in DMSO to a concentration of 2 mg/ml and subsequently diluted to the working concentrations in the desired buffers. Final concentration of DMSO in the peptide solutions ranged from 9% to 0.1% (v/v).

For one round of experiments, PSM α 2 was solubilized in 6M GuHCl in 10 mM MES buffer and subjected to size exclusion chromatography using a Superdex Peptide 10/300 GL column with absorbance measurements at 214 nm and 256 nm. The different elution fractions were collected in 10 mM Tris 50 mM NaCl buffer.

α -syn was either incubated on its own, in the presence of different concentrations of the PSM α peptides, or in the presence of DMSO. Most experiments were performed in 96-well black Corning polystyrene half-area microtiter plates with PEGylated surface (Corning 3881) in the presence of 20 μ M ThT and 0.01% NaN₃ under quiescent conditions. Replicates without ThT were also prepared for additions to cell cultures. For one experiment, 96-well polystyrene plates were instead used. For another, solutions were aliquoted into Eppendorf tubes and agitated at 1060 rpm. All aggregation experiments were performed at 37°C. Fluorescence was measured with an excitation filter of 440 nm and emission filter of 480 nm for up to 400h.

Analysis of Kinetics Data

The fluorescence measurements were normalized using Amylofit. Amylofit was also used to fit models of primary nucleation and elongation or of primary nucleation, elongation and secondary nucleation to the kinetics data of α -syn incubated on its own or in the presence of different concentrations of the PSM α peptides.

Electrophoresis and Mass Spectrometry

Samples of α -syn incubated on its own or in the presence of the PSM α peptides were size-separated on Novex 10–20% Tricine precast gels in Tris/Tricine SDS Running buffer (100 mM Tris base; 100 mM Tricine; 0.1% SDS; pH = 8.3). Gel bands were excised and subjected to in-gel digestion using 50 mM NH₄HCO₃ with 12 ng/ μ l sequencing-grade modified trypsin (Promega, Madison, WI, USA). Post trifluoroacetic acid addition, the digested peptide solutions were analyzed by MALDI TOF/TOF mass spectrometry.

Peptide arrays

Different 10-residue peptides corresponding to the PSM α sequences were immobilized on a microarray chip, washed and blocked in a solution of 3% (w/v)

skim milk in PBS with 0.1 % Tween-20 before it was probed with fluorescently labelled α -syn. After unbound α -syn was washed off, the array was scanned using a Typhoon Trio scanner (GE Life Sciences, Pittsburgh, PA, USA) and the fluorescence intensities quantified using ImageJ.

Transmission Electron Microscopy

The different aggregated samples were diluted 1:500 in PBS buffer and then added onto carbon-coated grids. The grids were washed in PBS and blocked with a BSA solution, then incubated with primary antibody solution (1:200 syn211), washed again and incubated with 10 nm gold-labelled anti-mouse antibody solution. The grids were washed again then fixed with glutaraldehyde and (Ted Pella 18427) and uranyl acetate (Agar Scientific R1260A, Essex, UK). Alternatively, the samples were not immunolabelled but only fixed with glutaraldehyde and uranyl acetate. Images were acquired using a FEI Tecnai Biotwin 120 kV Electron Microscope (Minnesota, MN, USA).

Dynamic Light Scattering

α -syn incubated on its own or in the presence of 2%, 5% or 10% DMSO (v/v) was aliquoted in disposable plastic cuvettes. A Wyatt Technology DynaPro NanoStar was used to measure the particle size, with laser strength set to 100% and scatter angle fixed to 90°. Ten consecutive 5 second measurements were compounded and analyzed.

Proteinase K digestion and Western Blotting

α -syn incubated on its own or in the presence of DMSO was pelleted at 25000g at 20°C and resuspended in PBS to remove the DMSO. 40 μ g of the resuspended α -syn was diluted 1:1 in digestion buffer and proteinase K added at final concentrations of 2, 10 and 50 μ g/ml. The samples were then incubated at 37°C for 30 minutes with slow agitation. The digestions were stopped with Pefabloc and left at room temperature for 10 minutes. The samples were then prepared for Western blotting by further dilution in SDS-loading buffer (1:1) and boiling for 5 minutes followed by vortexing. 30 minutes later the samples were again boiled for 5 minutes and size-separated on Novex 16% Tricine Gels which were stained using Coomassie Brilliant Blue.

Cell Culture

SH-SY5Y cells

We used a SH-SY5Y cell line stably overexpressing full-length wildtype human α -syn under the control of a Tet-Off-system, where α -syn expression can be suppressed by doxycycline (dox) treatment. The cell line was kindly provided by Professor, Dr. Leonidas Stefanis (Division of Basic Neurosciences, Biomedical Research Foundation of the Academy of Athens, Athens, Greece). The cells were maintained at 37°C under 5% CO₂ in RPMI 1640 medium with l-Glutamine (Lonza) supplemented with 15% fetal calf serum, 50 U/mL penicillin and 50 µg/mL streptomycin, 50 µg/mL hygromycin B (Invitrogen, LifeTechnologies), 200 µg/mL geneticin (VWR), 1 µg/mL dox (VWR), and 5 µg/mL Plasmocin. For experiments, cells were seeded without hygromycin B, geneticin, plasmocin.

DMSO treatment of SH-SY5Y cells

The SH-SY5Y cells were seeded onto poly-L-lysine coated coverslips and differentiated with 10 µM retinoic acid. Retinoic acid was included in the media for the duration of the experiment. Dox treatment was stopped 24 hours after seeding and DMSO simultaneously added. The cells were treated with DMSO for 7 consecutive days with medium renewal every other day. The cells were fixed, blocked and probed with primary antibodies against tubulin, a specific conformation of α -syn, and p-syn and fluorescently labelled secondary antibodies (anti-mouse and anti-rabbit) with dilutions as specified in Table 3. Nuclei were stained with DAPI.

Images were acquired on a Zeiss ObserverZ1 microscope.

HEK 293T Culture

HEK 293T cells stably transduced with the A53T variant of α -syn fused to GFP were maintained in DMEM GlutaMAX (Gibco 10569010, Texas, TX, USA) supplemented with 10% fetal bovine serum (Gibco 10270-106) and 1% penicillin-streptomycin (Gibco 15140-122) and split every three days.

Alpha-synuclein and PSM α treatment of HEK 293T cells

Cells were seeded onto collagen G-coated (Biochrom GmbH L7213, Berlin, Germany) black, clear bottom 96-well plates. Samples of co- or separately incubated α -syn and PSM α were sonicated at 100% amplitude for 3 min with 1 second on/1

second off cycles. 10 μ l of each sample was added in 4 or 3 replicates into 100 μ l medium. The plates were imaged for 48h with 1h intervals using a Nikon Ti-E microscope with 95% humidity 5% CO₂.

48 hours post initiation of the treatment, the cells were fixed, blocked and probed with an antibody against p-syn and a Cy3-conjugated anti-rabbit antibody. Images were acquired on the Nikon Ti-E microscope.

References

1. Marti MJ, Tolosa E, Campdelacreu J. Clinical overview of the synucleinopathies. *Mov Disord.* 2003;18 Suppl 6:S21-7.
2. Parkinson J. An essay on the shaking palsy. 1817. *J Neuropsychiatry Clin Neurosci.* 2002;14(2):223-36; discussion 2.
3. Boeve BF, Silber MH, Ferman TJ, Lucas JA, Parisi JE. Association of REM sleep behavior disorder and neurodegenerative disease may reflect an underlying synucleinopathy. *Mov Disord.* 2001;16(4):622-30.
4. Braak H, Del Tredici K. Neuropathological Staging of Brain Pathology in Sporadic Parkinson's disease: Separating the Wheat from the Chaff. *J Parkinsons Dis.* 2017;7(s1):S71-S85.
5. Braak H, Del Tredici K, Rub U, de Vos RA, Jansen Steur EN, Braak E. Staging of brain pathology related to sporadic Parkinson's disease. *Neurobiol Aging.* 2003;24(2):197-211.
6. Adler CH, Beach TG, Zhang N, Shill HA, Driver-Dunckley E, Caviness JN, et al. Unified Staging System for Lewy Body Disorders: Clinicopathologic Correlations and Comparison to Braak Staging. *J Neuropathol Exp Neurol.* 2019;78(10):891-9.
7. Marui W, Iseki E, Nakai T, Miura S, Kato M, Ueda K, et al. Progression and staging of Lewy pathology in brains from patients with dementia with Lewy bodies. *J Neurol Sci.* 2002;195(2):153-9.
8. Outeiro TF, Koss DJ, Erskine D, Walker L, Kurzawa-Akanbi M, Burn D, et al. Dementia with Lewy bodies: an update and outlook. *Mol Neurodegener.* 2019;14(1):5.
9. Halliday GM. Re-evaluating the glio-centric view of multiple system atrophy by highlighting the neuronal involvement. *Brain.* 2015;138(Pt 8):2116-9.
10. Maroteaux L, Campanelli JT, Scheller RH. Synuclein: a neuron-specific protein localized to the nucleus and presynaptic nerve terminal. *J Neurosci.* 1988;8(8):2804-15.
11. Ueda K, Fukushima H, Masliah E, Xia Y, Iwai A, Yoshimoto M, et al. Molecular cloning of cDNA encoding an unrecognized component of amyloid in Alzheimer disease. *Proc Natl Acad Sci U S A.* 1993;90(23):11282-6.
12. Polymeropoulos MH, Higgins JJ, Golbe LI, Johnson WG, Ide SE, Di Iorio G, et al. Mapping of a gene for Parkinson's disease to chromosome 4q21-q23. *Science.* 1996;274(5290):1197-9.
13. Spillantini MG, Schmidt ML, Lee VM, Trojanowski JQ, Jakes R, Goedert M. Alpha-synuclein in Lewy bodies. *Nature.* 1997;388(6645):839-40.

14. Spillantini MG, Crowther RA, Jakes R, Cairns NJ, Lantos PL, Goedert M. Filamentous alpha-synuclein inclusions link multiple system atrophy with Parkinson's disease and dementia with Lewy bodies. *Neurosci Lett*. 1998;251(3):205-8.
15. Wakabayashi K, Yoshimoto M, Tsuji S, Takahashi H. Alpha-synuclein immunoreactivity in glial cytoplasmic inclusions in multiple system atrophy. *Neurosci Lett*. 1998;249(2-3):180-2.
16. Scholz SW, Houlden H, Schulte C, Sharma M, Li A, Berg D, et al. SNCA variants are associated with increased risk for multiple system atrophy. *Ann Neurol*. 2009;65(5):610-4.
17. Whittaker HT, Qui Y, Bettencourt C, Houlden H. Multiple system atrophy: genetic risks and alpha-synuclein mutations. *F1000Res*. 2017;6:2072.
18. Siddiqui IJ, Pervaiz N, Abbasi AA. The Parkinson Disease gene SNCA: Evolutionary and structural insights with pathological implication. *Sci Rep*. 2016;6:24475.
19. Zarbiv Y, Simhi-Haham D, Israeli E, Elhadi SA, Grigoletto J, Sharon R. Lysine residues at the first and second KTKEGV repeats mediate alpha-Synuclein binding to membrane phospholipids. *Neurobiol Dis*. 2014;70:90-8.
20. Emamzadeh FN. Alpha-synuclein structure, functions, and interactions. *J Res Med Sci*. 2016;21:29.
21. Dettmer U. Rationally Designed Variants of alpha-Synuclein Illuminate Its in vivo Structural Properties in Health and Disease. *Front Neurosci*. 2018;12:623.
22. Logan T, Bendor J, Toupin C, Thorn K, Edwards RH. alpha-Synuclein promotes dilation of the exocytotic fusion pore. *Nat Neurosci*. 2017;20(5):681-9.
23. Burre J, Sharma M, Tsetsenis T, Buchman V, Etherton MR, Sudhof TC. Alpha-synuclein promotes SNARE-complex assembly in vivo and in vitro. *Science*. 2010;329(5999):1663-7.
24. Makasewicz K, Wennmalm S, Stenqvist B, Fornasier M, Andersson A, Jonsson P, et al. Cooperativity of alpha-Synuclein Binding to Lipid Membranes. *ACS Chem Neurosci*. 2021;12(12):2099-109.
25. Gretchen-Harrison B, Polydoro M, Morimoto-Tomita M, Diao L, Williams AM, Nie EH, et al. alphasynuclein triple knockout mice reveal age-dependent neuronal dysfunction. *Proc Natl Acad Sci U S A*. 2010;107(45):19573-8.
26. Kruger R, Kuhn W, Muller T, Woitalla D, Graeber M, Kosel S, et al. Ala30Pro mutation in the gene encoding alpha-synuclein in Parkinson's disease. *Nat Genet*. 1998;18(2):106-8.
27. Zarranz JJ, Alegre J, Gomez-Esteban JC, Lezcano E, Ros R, Ampuero I, et al. The new mutation, E46K, of alpha-synuclein causes Parkinson and Lewy body dementia. *Ann Neurol*. 2004;55(2):164-73.
28. Appel-Cresswell S, Vilarino-Guell C, Encarnacion M, Sherman H, Yu I, Shah B, et al. Alpha-synuclein p.H50Q, a novel pathogenic mutation for Parkinson's disease. *Mov Disord*. 2013;28(6):811-3.

29. Lesage S, Anheim M, Letournel F, Bousset L, Honore A, Rozas N, et al. G51D alpha-synuclein mutation causes a novel parkinsonian-pyramidal syndrome. *Ann Neurol*. 2013;73(4):459-71.
30. Polymeropoulos MH, Lavedan C, Leroy E, Ide SE, Dehejia A, Dutra A, et al. Mutation in the alpha-synuclein gene identified in families with Parkinson's disease. *Science*. 1997;276(5321):2045-7.
31. Pasanen P, Myllykangas L, Siitonen M, Raunio A, Kaakkola S, Lyytinen J, et al. Novel alpha-synuclein mutation A53E associated with atypical multiple system atrophy and Parkinson's disease-type pathology. *Neurobiol Aging*. 2014;35(9):2180 e1-5.
32. Yoshino H, Hirano M, Stoessl AJ, Imamichi Y, Ikeda A, Li Y, et al. Homozygous alpha-synuclein p.A53V in familial Parkinson's disease. *Neurobiol Aging*. 2017;57:248 e7- e12.
33. Ruf VC, Nubling GS, Willikens S, Shi S, Schmidt F, Levin J, et al. Different Effects of alpha-Synuclein Mutants on Lipid Binding and Aggregation Detected by Single Molecule Fluorescence Spectroscopy and ThT Fluorescence-Based Measurements. *ACS Chem Neurosci*. 2019;10(3):1649-59.
34. Flagmeier P, Meisl G, Vendruscolo M, Knowles TP, Dobson CM, Buell AK, et al. Mutations associated with familial Parkinson's disease alter the initiation and amplification steps of alpha-synuclein aggregation. *Proc Natl Acad Sci U S A*. 2016;113(37):10328-33.
35. Rovere M, Powers AE, Jiang H, Pitino JC, Fonseca-Ornelas L, Patel DS, et al. E46K-like alpha-synuclein mutants increase lipid interactions and disrupt membrane selectivity. *J Biol Chem*. 2019;294(25):9799-812.
36. Ghio S, Camilleri A, Caruana M, Ruf VC, Schmidt F, Leonov A, et al. Cardiolipin Promotes Pore-Forming Activity of Alpha-Synuclein Oligomers in Mitochondrial Membranes. *ACS Chem Neurosci*. 2019;10(8):3815-29.
37. Martinez JH, Alaimo A, Gorjod RM, Porte Alcon S, Fuentes F, Coluccio Leskow F, et al. Drp-1 dependent mitochondrial fragmentation and protective autophagy in dopaminergic SH-SY5Y cells overexpressing alpha-synuclein. *Mol Cell Neurosci*. 2018;88:107-17.
38. Faustini G, Bono F, Valerio A, Pizzi M, Spano P, Bellucci A. Mitochondria and alpha-Synuclein: Friends or Foes in the Pathogenesis of Parkinson's Disease? *Genes (Basel)*. 2017;8(12).
39. McKinnon C, De Snoo ML, Gondard E, Neudorfer C, Chau H, Ngana SG, et al. Early-onset impairment of the ubiquitin-proteasome system in dopaminergic neurons caused by alpha-synuclein. *Acta Neuropathol Commun*. 2020;8(1):17.
40. Mazzulli JR, Zunke F, Isacson O, Studer L, Krainc D. alpha-Synuclein-induced lysosomal dysfunction occurs through disruptions in protein trafficking in human midbrain synucleinopathy models. *Proc Natl Acad Sci U S A*. 2016;113(7):1931-6.
41. Ulmer TS, Bax A, Cole NB, Nussbaum RL. Structure and dynamics of micelle-bound human alpha-synuclein. *J Biol Chem*. 2005;280(10):9595-603.

42. Tuttle MD, Comellas G, Nieuwkoop AJ, Covell DJ, Berthold DA, Kloepper KD, et al. Solid-state NMR structure of a pathogenic fibril of full-length human alpha-synuclein. *Nat Struct Mol Biol.* 2016;23(5):409-15.
43. Sehnaal D, Bittrich S, Deshpande M, Svobodova R, Berka K, Bazgier V, et al. Mol* Viewer: modern web app for 3D visualization and analysis of large biomolecular structures. *Nucleic Acids Res.* 2021;49(W1):W431-W7.
44. Bartels T, Choi JG, Selkoe DJ. alpha-Synuclein occurs physiologically as a helically folded tetramer that resists aggregation. *Nature.* 2011;477(7362):107-10.
45. Linse S. Monomer-dependent secondary nucleation in amyloid formation. *Biophys Rev.* 2017;9(4):329-38.
46. Bousset L, Pieri L, Ruiz-Arlandis G, Gath J, Jensen PH, Habenstein B, et al. Structural and functional characterization of two alpha-synuclein strains. *Nat Commun.* 2013;4:2575.
47. Peduzzo A, Linse S, Buell AK. The Properties of alpha-Synuclein Secondary Nuclei Are Dominated by the Solution Conditions Rather than the Seed Fibril Strain. *ACS Chem Neurosci.* 2020;11(6):909-18.
48. Le Dur A, Lai TL, Stinnakre MG, Laisne A, Chenais N, Rakotobe S, et al. Divergent prion strain evolution driven by PrP(C) expression level in transgenic mice. *Nat Commun.* 2017;8:14170.
49. Kordower JH, Chu Y, Hauser RA, Freeman TB, Olanow CW. Lewy body-like pathology in long-term embryonic nigral transplants in Parkinson's disease. *Nat Med.* 2008;14(5):504-6.
50. Li JY, Englund E, Holton JL, Soulet D, Hagell P, Lees AJ, et al. Lewy bodies in grafted neurons in subjects with Parkinson's disease suggest host-to-graft disease propagation. *Nat Med.* 2008;14(5):501-3.
51. Braak H, Rub U, Gai WP, Del Tredici K. Idiopathic Parkinson's disease: possible routes by which vulnerable neuronal types may be subject to neuroinvasion by an unknown pathogen. *J Neural Transm (Vienna).* 2003;110(5):517-36.
52. Beck G, Hori Y, Hayashi Y, Morii E, Takehara T, Mochizuki H. Detection of Phosphorylated Alpha-Synuclein in the Muscularis Propria of the Gastrointestinal Tract Is a Sensitive Predictor for Parkinson's Disease. *Parkinsons Dis.* 2020;2020:4687530.
53. Svensson E, Horvath-Puho E, Thomsen RW, Djurhuus JC, Pedersen L, Borghammer P, et al. Vagotomy and subsequent risk of Parkinson's disease. *Ann Neurol.* 2015;78(4):522-9.
54. Holmqvist S, Chutna O, Bousset L, Aldrin-Kirk P, Li W, Bjorklund T, et al. Direct evidence of Parkinson pathology spread from the gastrointestinal tract to the brain in rats. *Acta Neuropathol.* 2014;128(6):805-20.
55. Lohmann S, Bernis ME, Tachu BJ, Ziemski A, Grigoletto J, Tamguney G. Oral and intravenous transmission of alpha-synuclein fibrils to mice. *Acta Neuropathol.* 2019;138(4):515-33.
56. Rey NL, Petit GH, Bousset L, Melki R, Brundin P. Transfer of human alpha-synuclein from the olfactory bulb to interconnected brain regions in mice. *Acta Neuropathol.* 2013;126(4):555-73.

57. Rey NL, Steiner JA, Maroof N, Luk KC, Madaj Z, Trojanowski JQ, et al. Widespread transneuronal propagation of alpha-synucleinopathy triggered in olfactory bulb mimics prodromal Parkinson's disease. *J Exp Med*. 2016;213(9):1759-78.
58. Rey NL, George S, Steiner JA, Madaj Z, Luk KC, Trojanowski JQ, et al. Spread of aggregates after olfactory bulb injection of alpha-synuclein fibrils is associated with early neuronal loss and is reduced long term. *Acta Neuropathol*. 2018;135(1):65-83.
59. Peng C, Gathagan RJ, Covell DJ, Medellin C, Stieber A, Robinson JL, et al. Cellular milieu imparts distinct pathological alpha-synuclein strains in alpha-synucleinopathies. *Nature*. 2018;557(7706):558-63.
60. Berry C, La Vecchia C, Nicotera P. Paraquat and Parkinson's disease. *Cell Death Differ*. 2010;17(7):1115-25.
61. Langston JW, Ballard P, Tetrud JW, Irwin I. Chronic Parkinsonism in humans due to a product of meperidine-analog synthesis. *Science*. 1983;219(4587):979-80.
62. Zhu F, Li C, Gong J, Zhu W, Gu L, Li N. The risk of Parkinson's disease in inflammatory bowel disease: A systematic review and meta-analysis. *Dig Liver Dis*. 2019;51(1):38-42.
63. Hui KY, Fernandez-Hernandez H, Hu J, Schaffner A, Pankratz N, Hsu NY, et al. Functional variants in the LRRK2 gene confer shared effects on risk for Crohn's disease and Parkinson's disease. *Sci Transl Med*. 2018;10(423).
64. Haikal C, Chen QQ, Li JY. Microbiome changes: an indicator of Parkinson's disease? *Transl Neurodegener*. 2019;8:38.
65. Sampson TR, Debelius JW, Thron T, Janssen S, Shastri GG, Ilhan ZE, et al. Gut Microbiota Regulate Motor Deficits and Neuroinflammation in a Model of Parkinson's Disease. *Cell*. 2016;167(6):1469-80 e12.
66. Kohbata S, Beaman BL. L-dopa-responsive movement disorder caused by *Nocardia asteroides* localized in the brains of mice. *Infect Immun*. 1991;59(1):181-91.
67. Caldwell KA, Tucci ML, Armagost J, Hodges TW, Chen J, Memon SB, et al. Investigating bacterial sources of toxicity as an environmental contributor to dopaminergic neurodegeneration. *PLoS One*. 2009;4(10):e7227.
68. Chorell E, Andersson E, Evans ML, Jain N, Gotheson A, Aden J, et al. Bacterial Chaperones CsgE and CsgC Differentially Modulate Human alpha-Synuclein Amyloid Formation via Transient Contacts. *PLoS One*. 2015;10(10):e0140194.
69. Chen SG, Stribinskis V, Rane MJ, Demuth DR, Gozal E, Roberts AM, et al. Exposure to the Functional Bacterial Amyloid Protein Curli Enhances Alpha-Synuclein Aggregation in Aged Fischer 344 Rats and *Caenorhabditis elegans*. *Sci Rep*. 2016;6:34477.
70. Little CS, Hammond CJ, MacIntyre A, Balin BJ, Appelt DM. Chlamydia pneumoniae induces Alzheimer-like amyloid plaques in brains of BALB/c mice. *Neurobiol Aging*. 2004;25(4):419-29.
71. Eimer WA, Vijaya Kumar DK, Navalpur Shanmugam NK, Rodriguez AS, Mitchell T, Washicosky KJ, et al. Alzheimer's Disease-Associated beta-Amyloid Is Rapidly Seeded by Herpesviridae to Protect against Brain Infection. *Neuron*. 2018;100(6):1527-32.

72. Ezzat K, Pernemalm M, Palsson S, Roberts TC, Jarver P, Dondalska A, et al. The viral protein corona directs viral pathogenesis and amyloid aggregation. *Nat Commun.* 2019;10(1):2331.
73. Park SC, Moon JC, Shin SY, Son H, Jung YJ, Kim NH, et al. Functional characterization of alpha-synuclein protein with antimicrobial activity. *Biochem Biophys Res Commun.* 2016;478(2):924-8.
74. Beatman EL, Massey A, Shives KD, Burrack KS, Chamanian M, Morrison TE, et al. Alpha-Synuclein Expression Restricts RNA Viral Infections in the Brain. *J Virol.* 2015;90(6):2767-82.
75. Tomlinson JJ, Shutinoski B, Dong L, Meng F, Elleithy D, Lengacher NA, et al. Holocranohistochemistry enables the visualization of alpha-synuclein expression in the murine olfactory system and discovery of its systemic anti-microbial effects. *J Neural Transm (Vienna).* 2017;124(6):721-38.
76. Chiu IM, Heesters BA, Ghasemlou N, Von Hehn CA, Zhao F, Tran J, et al. Bacteria activate sensory neurons that modulate pain and inflammation. *Nature.* 2013;501(7465):52-7.
77. Pinho-Ribeiro FA, Baddal B, Haarsma R, O'Seaghdha M, Yang NJ, Blake KJ, et al. Blocking Neuronal Signaling to Immune Cells Treats Streptococcal Invasive Infection. *Cell.* 2018;173(5):1083-97 e22.
78. Kashem SW, Riedl MS, Yao C, Honda CN, Vulchanova L, Kaplan DH. Nociceptive Sensory Fibers Drive Interleukin-23 Production from CD301b+ Dermal Dendritic Cells and Drive Protective Cutaneous Immunity. *Immunity.* 2015;43(3):515-26.
79. Soscia SJ, Kirby JE, Washicosky KJ, Tucker SM, Ingelsson M, Hyman B, et al. The Alzheimer's disease-associated amyloid beta-protein is an antimicrobial peptide. *PLoS One.* 2010;5(3):e9505.
80. Kumar DK, Choi SH, Washicosky KJ, Eimer WA, Tucker S, Ghofrani J, et al. Amyloid-beta peptide protects against microbial infection in mouse and worm models of Alzheimer's disease. *Sci Transl Med.* 2016;8(340):340ra72.
81. Balin BJ, Gerard HC, Arking EJ, Appelt DM, Branigan PJ, Abrams JT, et al. Identification and localization of Chlamydia pneumoniae in the Alzheimer's brain. *Med Microbiol Immunol.* 1998;187(1):23-42.
82. Itzhaki RF, Lin WR, Shang D, Wilcock GK, Faragher B, Jamieson GA. Herpes simplex virus type 1 in brain and risk of Alzheimer's disease. *Lancet.* 1997;349(9047):241-4.
83. Jamieson GA, Maitland NJ, Wilcock GK, Craske J, Itzhaki RF. Latent herpes simplex virus type 1 in normal and Alzheimer's disease brains. *J Med Virol.* 1991;33(4):224-7.
84. Miklossy J. Alzheimer's disease--a spirochetosis? *Neuroreport.* 1993;4(7):841-8.
85. Alonso R, Pisa D, Aguado B, Carrasco L. Identification of Fungal Species in Brain Tissue from Alzheimer's Disease by Next-Generation Sequencing. *J Alzheimers Dis.* 2017;58(1):55-67.
86. Alonso R, Pisa D, Fernandez-Fernandez AM, Carrasco L. Infection of Fungi and Bacteria in Brain Tissue From Elderly Persons and Patients With Alzheimer's Disease. *Front Aging Neurosci.* 2018;10:159.

87. Pisa D, Alonso R, Fernandez-Fernandez AM, Rabano A, Carrasco L. Polymicrobial Infections In Brain Tissue From Alzheimer's Disease Patients. *Sci Rep*. 2017;7(1):5559.
88. Pisa D, Alonso R, Carrasco L. Parkinson's Disease: A Comprehensive Analysis of Fungi and Bacteria in Brain Tissue. *Int J Biol Sci*. 2020;16(7):1135-52.
89. Bjornevik K, Cortese M, Healy BC, Kuhle J, Mina MJ, Leng Y, et al. Longitudinal analysis reveals high prevalence of Epstein-Barr virus associated with multiple sclerosis. *Science*. 2022;375(6578):296-301.
90. Weitzman MD, Weitzman JB. What's the damage? The impact of pathogens on pathways that maintain host genome integrity. *Cell Host Microbe*. 2014;15(3):283-94.
91. Gordevicius J, Li P, Marshall LL, Killinger BA, Lang S, Ensink E, et al. Epigenetic inactivation of the autophagy-lysosomal system in appendix in Parkinson's disease. *Nat Commun*. 2021;12(1):5134.
92. Schaser AJ, Osterberg VR, Dent SE, Stackhouse TL, Wakeham CM, Boutros SW, et al. Alpha-synuclein is a DNA binding protein that modulates DNA repair with implications for Lewy body disorders. *Sci Rep*. 2019;9(1):10919.
93. Ma L, Yang C, Zhang X, Li Y, Wang S, Zheng L, et al. C-terminal truncation exacerbates the aggregation and cytotoxicity of alpha-Synuclein: A vicious cycle in Parkinson's disease. *Biochim Biophys Acta Mol Basis Dis*. 2018;1864(12):3714-25.
94. Lim S, Chun Y, Lee JS, Lee SJ. Neuroinflammation in Synucleinopathies. *Brain Pathol*. 2016;26(3):404-9.
95. Shameli A, Xiao W, Zheng Y, Shyu S, Sumodi J, Meyerson HJ, et al. A critical role for alpha-synuclein in development and function of T lymphocytes. *Immunobiology*. 2016;221(2):333-40.
96. Brochard V, Combadiere B, Prigent A, Laouar Y, Perrin A, Beray-Berthet V, et al. Infiltration of CD4⁺ lymphocytes into the brain contributes to neurodegeneration in a mouse model of Parkinson disease. *J Clin Invest*. 2009;119(1):182-92.
97. Sommer A, Fadler T, Dorfmeister E, Hoffmann AC, Xiang W, Winner B, et al. Infiltrating T lymphocytes reduce myeloid phagocytosis activity in synucleinopathy model. *J Neuroinflammation*. 2016;13(1):174.
98. George S, Tyson T, Rey NL, Sheridan R, Peelaerts W, Becker K, et al. T Cells Limit Accumulation of Aggregate Pathology Following Intrastratial Injection of alpha-Synuclein Fibrils. *J Parkinsons Dis*. 2021;11(2):585-603.
99. Nissen SK, Shrivastava K, Schulte C, Otzen DE, Goldeck D, Berg D, et al. Alterations in Blood Monocyte Functions in Parkinson's Disease. *Mov Disord*. 2019;34(11):1711-21.
100. Baba Y, Kuroiwa A, Uitti RJ, Wszolek ZK, Yamada T. Alterations of T-lymphocyte populations in Parkinson disease. *Parkinsonism Relat Disord*. 2005;11(8):493-8.
101. Hisanaga K, Asagi M, Itoyama Y, Iwasaki Y. Increase in peripheral CD4 bright⁺ CD8 dull⁺ T cells in Parkinson disease. *Arch Neurol*. 2001;58(10):1580-3.

102. Lindestam Arlehamn CS, Dhanwani R, Pham J, Kuan R, Frazier A, Rezende Dutra J, et al. alpha-Synuclein-specific T cell reactivity is associated with preclinical and early Parkinson's disease. *Nat Commun.* 2020;11(1):1875.
103. Bonaz B, Sinniger V, Pellissier S. The Vagus Nerve in the Neuro-Immune Axis: Implications in the Pathology of the Gastrointestinal Tract. *Front Immunol.* 2017;8:1452.
104. Liu S, da Cunha AP, Rezende RM, Cialic R, Wei Z, Bry L, et al. The Host Shapes the Gut Microbiota via Fecal MicroRNA. *Cell Host Microbe.* 2016;19(1):32-43.
105. Hewel C, Kaiser J, Wierczeiko A, Linke J, Reinhardt C, Endres K, et al. Common miRNA Patterns of Alzheimer's Disease and Parkinson's Disease and Their Putative Impact on Commensal Gut Microbiota. *Front Neurosci.* 2019;13:113.
106. Luk KC, Mills IP, Trojanowski JQ, Lee VM. Interactions between Hsp70 and the hydrophobic core of alpha-synuclein inhibit fibril assembly. *Biochemistry.* 2008;47(47):12614-25.
107. Gao X, Carroni M, Nussbaum-Krammer C, Mogk A, Nillegoda NB, Szlachet A, et al. Human Hsp70 Disaggregase Reverses Parkinson's-Linked alpha-Synuclein Amyloid Fibrils. *Mol Cell.* 2015;59(5):781-93.
108. Wentink AS, Nillegoda NB, Feufel J, Ubartaite G, Schneider CP, De Los Rios P, et al. Molecular dissection of amyloid disaggregation by human HSP70. *Nature.* 2020;587(7834):483-8.
109. Cabrera M, Boronat S, Marte L, Vega M, Perez P, Ayte J, et al. Chaperone-Facilitated Aggregation of Thermo-Sensitive Proteins Shields Them from Degradation during Heat Stress. *Cell Rep.* 2020;30(7):2430-43 e4.
110. McFarthing K, Buff S, Rafaloff G, Dominey T, Wyse RK, Stott SRW. Parkinson's Disease Drug Therapies in the Clinical Trial Pipeline: 2020. *J Parkinsons Dis.* 2020;10(3):757-74.
111. Beyer K. Alpha-synuclein structure, posttranslational modification and alternative splicing as aggregation enhancers. *Acta Neuropathol.* 2006;112(3):237-51.
112. Gamez-Valero A, Beyer K. Alternative Splicing of Alpha- and Beta-Synuclein Genes Plays Differential Roles in Synucleinopathies. *Genes (Basel).* 2018;9(2).
113. Sorrentino ZA, Vijayaraghavan N, Gorion KM, Riffe CJ, Strang KH, Caldwell J, et al. Physiological C-terminal truncation of alpha-synuclein potentiates the prion-like formation of pathological inclusions. *J Biol Chem.* 2018;293(49):18914-32.
114. Terada M, Suzuki G, Nonaka T, Kametani F, Tamaoka A, Hasegawa M. The effect of truncation on prion-like properties of alpha-synuclein. *J Biol Chem.* 2018;293(36):13910-20.
115. Anderson JP, Walker DE, Goldstein JM, de Laat R, Banducci K, Caccavello RJ, et al. Phosphorylation of Ser-129 is the dominant pathological modification of alpha-synuclein in familial and sporadic Lewy body disease. *J Biol Chem.* 2006;281(40):29739-52.
116. Wang W, Nguyen LT, Burlak C, Chugini F, Guo F, Chataway T, et al. Caspase-1 causes truncation and aggregation of the Parkinson's disease-associated protein alpha-synuclein. *Proc Natl Acad Sci U S A.* 2016;113(34):9587-92.

117. Konnova EA, Swanberg M. Animal Models of Parkinson's Disease. In: Stoker TB, Greenland JC, editors. *Parkinson's Disease: Pathogenesis and Clinical Aspects*. Brisbane (AU)2018.
118. Dawson TM, Ko HS, Dawson VL. Genetic animal models of Parkinson's disease. *Neuron*. 2010;66(5):646-61.
119. Hansen C, Bjorklund T, Petit GH, Lundblad M, Murmu RP, Brundin P, et al. A novel alpha-synuclein-GFP mouse model displays progressive motor impairment, olfactory dysfunction and accumulation of alpha-synuclein-GFP. *Neurobiol Dis*. 2013;56:145-55.
120. Katorcha E, Makarava N, Lee YJ, Lindberg I, Monteiro MJ, Kovacs GG, et al. Cross-seeding of prions by aggregated alpha-synuclein leads to transmissible spongiform encephalopathy. *PLoS Pathog*. 2017;13(8):e1006563.
121. Ono K, Takahashi R, Ikeda T, Yamada M. Cross-seeding effects of amyloid beta-protein and alpha-synuclein. *J Neurochem*. 2012;122(5):883-90.
122. Waxman EA, Giasson BI. Induction of intracellular tau aggregation is promoted by alpha-synuclein seeds and provides novel insights into the hyperphosphorylation of tau. *J Neurosci*. 2011;31(21):7604-18.
123. Romero D, Kolter R. Functional amyloids in bacteria. *Int Microbiol*. 2014;17(2):65-73.
124. Besingi RN, Wenderska IB, Senadheera DB, Cvitkovitch DG, Long JR, Wen ZT, et al. Functional amyloids in *Streptococcus mutans*, their use as targets of biofilm inhibition and initial characterization of SMU_63c. *Microbiology (Reading)*. 2017;163(4):488-501.
125. Bjornsdottir H, Dahlstrand Rudin A, Klose FP, Elmwall J, Welin A, Stylianou M, et al. Phenol-Soluble Modulins alpha Peptide Toxins from Aggressive *Staphylococcus aureus* Induce Rapid Formation of Neutrophil Extracellular Traps through a Reactive Oxygen Species-Independent Pathway. *Front Immunol*. 2017;8:257.
126. Oppong GO, Rapsinski GJ, Tursi SA, Biesecker SG, Klein-Szanto AJ, Goulian M, et al. Biofilm-associated bacterial amyloids dampen inflammation in the gut: oral treatment with curli fibres reduces the severity of hapten-induced colitis in mice. *NPJ Biofilms Microbiomes*. 2015;1.
127. Wang R, Braughton KR, Kretschmer D, Bach TH, Queck SY, Li M, et al. Identification of novel cytolytic peptides as key virulence determinants for community-associated MRSA. *Nat Med*. 2007;13(12):1510-4.
128. Nakagawa S, Matsumoto M, Katayama Y, Oguma R, Wakabayashi S, Nygaard T, et al. *Staphylococcus aureus* Virulent PSMalpha Peptides Induce Keratinocyte Alarmin Release to Orchestrate IL-17-Dependent Skin Inflammation. *Cell Host Microbe*. 2017;22(5):667-77 e5.
129. Wu X, Yang M, Fang X, Zhen S, Zhang J, Yang X, et al. Expression and regulation of phenol-soluble modulins and enterotoxins in foodborne *Staphylococcus aureus*. *AMB Express*. 2018;8(1):187.
130. Blake KJ, Baral P, Voisin T, Lubkin A, Pinho-Ribeiro FA, Adams KL, et al. *Staphylococcus aureus* produces pain through pore-forming toxins and neuronal TRPV1 that is silenced by QX-314. *Nat Commun*. 2018;9(1):37.

131. Azevedo EP, Guimaraes-Costa AB, Torezani GS, Braga CA, Palhano FL, Kelly JW, et al. Amyloid fibrils trigger the release of neutrophil extracellular traps (NETs), causing fibril fragmentation by NET-associated elastase. *J Biol Chem.* 2012;287(44):37206-18.
132. Hogen T, Levin J, Schmidt F, Caruana M, Vassallo N, Kretzschmar H, et al. Two different binding modes of alpha-synuclein to lipid vesicles depending on its aggregation state. *Biophys J.* 2012;102(7):1646-55.
133. Duarte AM, van Mierlo CP, Hemminga MA. Molecular dynamics study of the solvation of an alpha-helical transmembrane peptide by DMSO. *J Phys Chem B.* 2008;112(29):8664-71.
134. Tanaka Y, Kubota A, Matsuo A, Kawakami A, Kamizi H, Mochigoe A, et al. Effect of Absorption Behavior of Solubilizers on Drug Dissolution in the Gastrointestinal Tract: Evaluation Based on In Vivo Luminal Concentration-Time Profile of Cilostazol, a Poorly Soluble Drug, and Solubilizers. *J Pharm Sci.* 2016;105(9):2825-31.
135. Kaplan JB, Izano EA, Gopal P, Karwacki MT, Kim S, Bose JL, et al. Low levels of beta-lactam antibiotics induce extracellular DNA release and biofilm formation in *Staphylococcus aureus*. *mBio.* 2012;3(4):e00198-12.
136. Grey M, Linse S, Nilsson H, Brundin P, Sparr E. Membrane interaction of alpha-synuclein in different aggregation states. *J Parkinsons Dis.* 2011;1(4):359-71.

Acknowledgements

It is not an easy task to put into words the gratitude I feel towards so many people, but I will make an attempt nonetheless.

Jia-Yi, I truly cannot imagine a better supervisor than you have been over these past years. I am so overcome with gratitude that I have been so fortunate to have you guide me through this PhD. I am repeatedly overwhelmed by how much more I have to learn from you, even though I have spent many years doing only that! Beyond your impressive expertise within the field, your passion for science shines through in your excitement for new projects and your commitment to high quality research. That you continuously and consistently have valued my ideas and shown patience during my learning process has built my confidence in my own abilities as a scientist, and for that I am forever grateful.

Sara, I am sure you have no shortage of people telling you that you are an inspiration to them, and I will happily be one of the masses. That everyone who has worked with you speaks firstly of your kindness, despite your long list of merits, is a testament to your character and truly something to aspire to.

The both of you have taught me the importance of humility in the pursuit of knowledge and the joys of this immeasurable privilege of being able to work with the motivation of satisfying one's own curiosity. It has been a true joy to work with the two of you!

I have crossed paths with many superstars but none that shine so brightly as Alicja Flasch. It's an honor to have learnt under your guidance and a joy to have spent time with you! Catarina Blennow, Ann-Charlotte Selberg, Anna-Karin Oldén, Marianne Juhlin, Susanne Jonsson, Birgitta Frohm, and Lina Gefors, you are the heroes that keep these labs working and I do not know of anyone who could have done it better than you!

My colleagues, friends and family, if I were to put into words everything I am grateful for I'd need another 5 years. Let me instead promise to continuously show you appreciation, as long as we may know each other.

Finally, I want to express gratitude towards the infinite mysteries of life. That, as surely as the sun will rise tomorrow, we will have questions to ponder and answers to seek, is a comfort in this vast world.



FACULTY OF MEDICINE

Dept of Experimental Medical Science
Neural Plasticity and Repair Unit

Lund University, Faculty of Medicine
Doctoral Dissertation Series 2022:40
ISBN 978-91-8021-201-4
ISSN 1652-8220

